

Chapter 1

Simulation of Residual Mechanical Capabilities Of ASR and DEF Expanded Concrete

1.1 General

In this chapter, three-dimensional expanded concrete models are tested under uni-axial compression condition, and the mechanical properties obtained from simulation are compared with previous experimental results from other researchers.

The purpose of this study is for the prediction of the behavior and residual capacity of ASR or DEF expanded concrete, especially in uni-axial compression.

1.2 Uni-axial compression result for 10x10x10mm Expanded Models

1.2.1 Uni-axial compression result for 10x10x10mm ASR Expanded Models

In this section, simulation uni-axial compression test on a single aggregate case in size only 10x10x10mm is presented. Displacement of loading boundary is controlled in this analysis. In each step of loading, the top boundary of the concrete model moves downwards 0.002mm.

It is easier to analyze the behavior under loading condition in very small scale around coarse aggregate in a relatively smaller model.

The model is expanded by ASR following the process in chapter 2 and 3. 0.001 initial strain is introduced in each step at the interfaces between the aggregate and paste elements. Totally 20 steps of expansion are done.

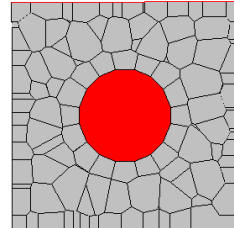


FIGURE 1.1: Single Aggregate Case in Size 10x10x10mm

For Loading with fixed boundary condition, Figure 1.2 here shows the initial stress condition during loading in loading step 0, 20, 30, 60 and 80.

With increasing the step of loading, in each step the top surface moves downwards for 0.002mm. Compressive strength generate together with the deformation, especially concentrated horizontally in the middle of the model.

As the top and bottom boundary are horizontally, elements in the middle of model start to move away from the center of model firstly, followed by the failure of whole model.

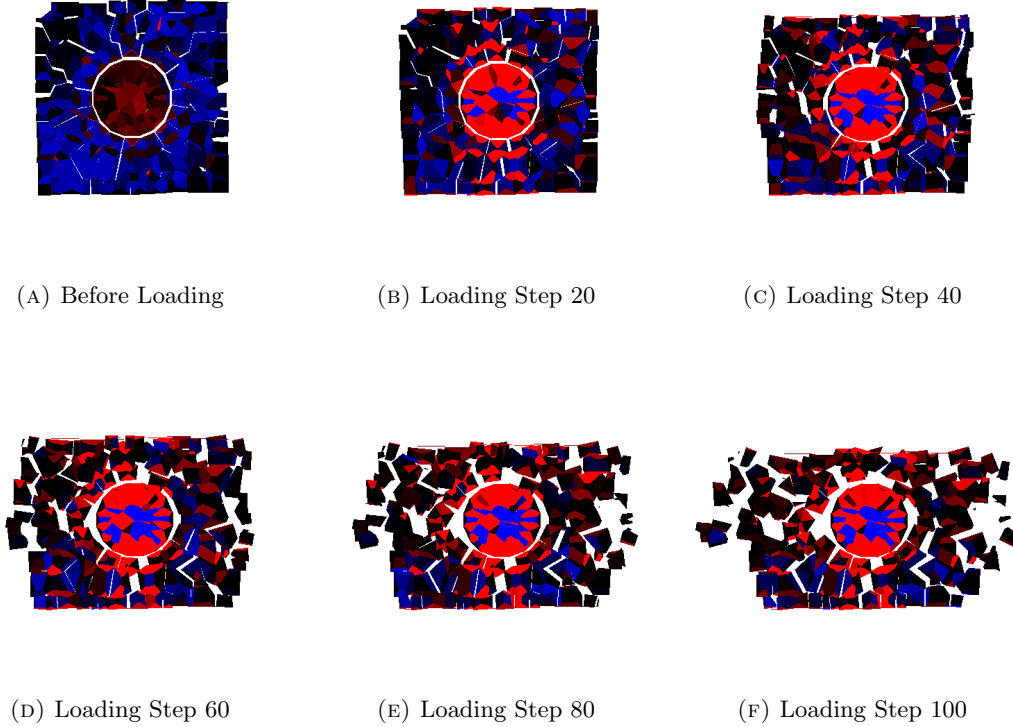


FIGURE 1.2: ASR Loading for 10x10x10mm model, Fixed Boundary Condition

If we compare its behavior with free boundary condition loading, shown in Figure 1.3, it can be seen that the way crack generate and deformation generate is totally different in these two cases.

In Free boundary loading, the cracks are more easier to open without the restrain from top and bottom boundary. The deformation in horizontal direction is more uniformed. Inner Stress distributed more uniformly in the free boundary loading case.

From the small size model it can be confirmed the workability of uni-axial compression test on a single aggregate 10x10x10mm model. Later, uni-axial compression test on full size model(100x100x100mm) damaged by ASR expansion will be carried out.

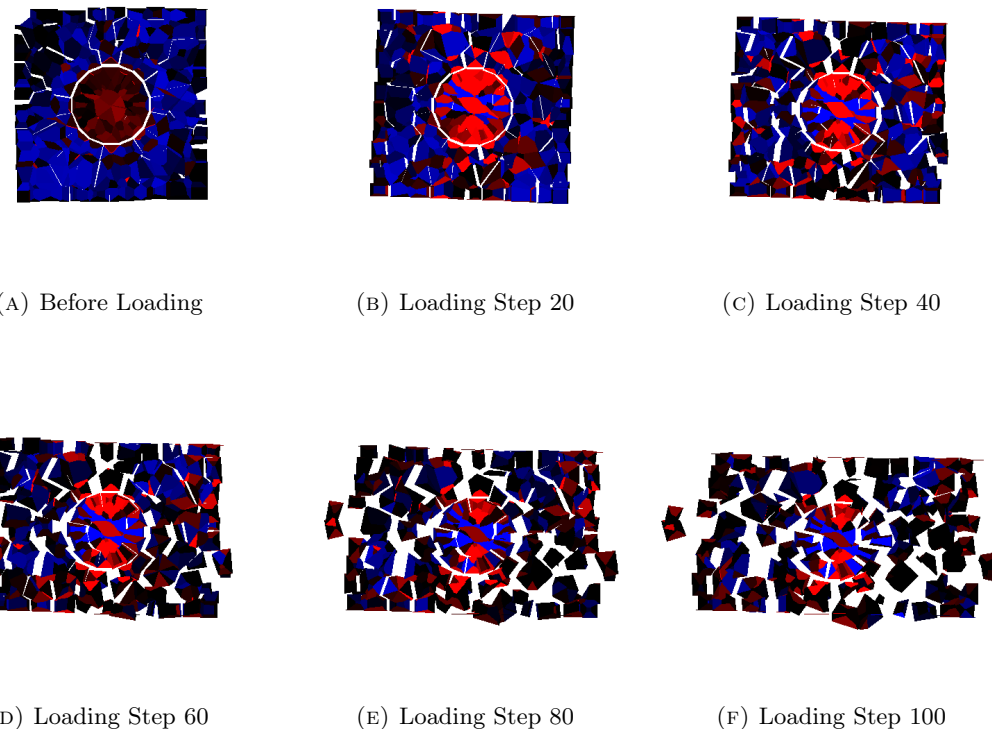


FIGURE 1.3: ASR Loading for 10x10x10mm model, Free Boundary Condition

1.2.2 Uni-axial compression result for 10x10x10mm DEF Expanded Models

Simulation of uni-axial compression test on a single aggregate case in size 10x10x10mm is presented also for DEF damaged concrete model. Same as in ASR case, in each step of loading, the top boundary of the concrete model moves downwards 0.002mm.

The model is expanded by DEF following the process in chapter 2 and 3. 0.0003 initial strain is given to all paste interfaces uniformly in this simulation. Totally 20 steps of expansion are done.

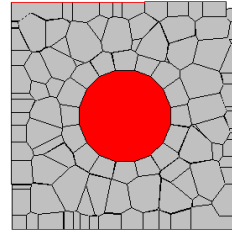


FIGURE 1.4: Single Aggregate Case in Size 10x10x10mm

For Loading with fixed boundary condition, Figure 1.5 here shows the initial stress condition during loading in loading step 0, 20, 30, 60 and 80.

With increasing the step of loading, in each step the top surface moves downwards for 0.002mm. Compressive strength generate together with the deformation, especially concentrated horizontally in the middle of the model.

As the top and bottom boundary are horizontally, elements in the middle of model start to move away from the center of model firstly, followed by the failure of whole model.

If we compare its behavior with free boundary condition loading, shown in Figure 1.6, it can be seen that the way crack generate and deformation generate is totally different in these two cases.

In Free boundary loading, the cracks are more easier to open without the restrain from top and bottom boundary. The deformation in horizontal direction is more uniformed. Inner Stress distributed more uniformly in the free boundary loading case.

Later, uni-axial compression test on full size model(100x100x100mm) damaged by DEF expansion will also be carried out.

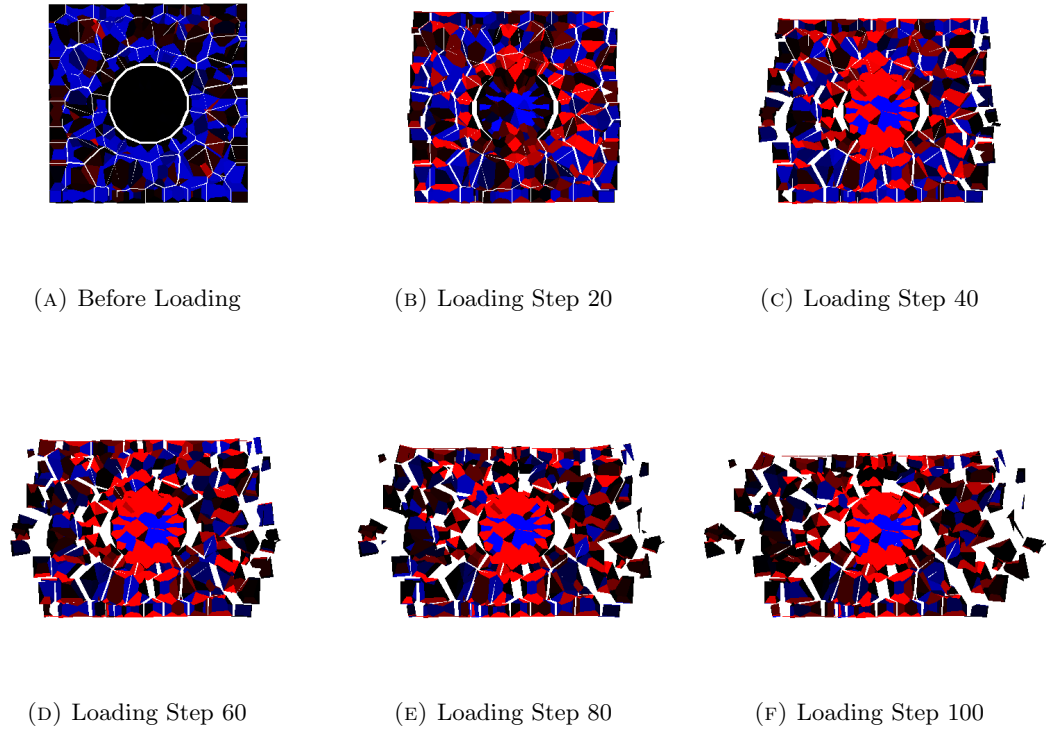


FIGURE 1.5: DEF Loading for 10x10x10mm model, Fixed Boundary Condition

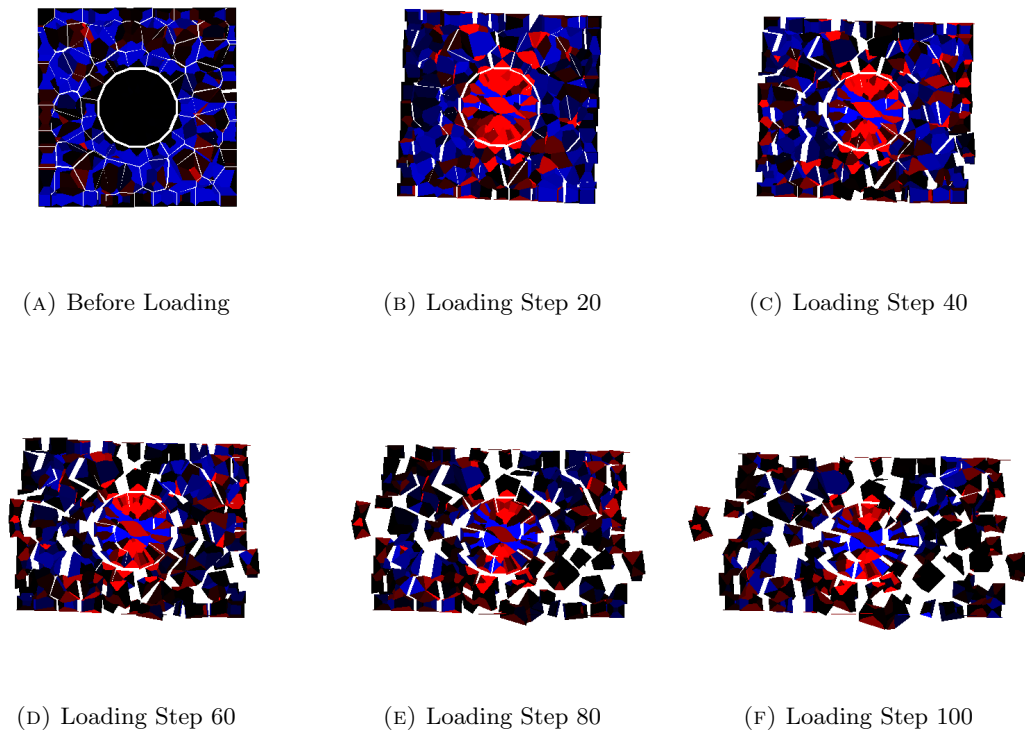


FIGURE 1.6: DEF Loading for 10x10x10mm model, Free Boundary Condition

1.3 Uni-axial compression result for 100x100x100mm Expanded Models

Displacement of loading boundary is controlled in this analysis. In each step of loading, the top boundary of the concrete model moves downwards 0.02mm.

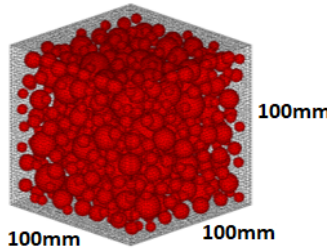


FIGURE 1.7: 30% Coarse Aggregate

Figure 1.8 and Figure 1.9 here presented the internal stress condition of 2 example cases for ASR and DEF loading of Fixed boundary condition, separately. In Figure , 100x100x100mm model with 30% coarse aggregate is used, of which 75% of all coarse aggregates are ASR reactive. While for DEF, same 100x100x100mm model with 30% coarse aggregate is used, of which the center 75x75x75mm part has been given intensified DEF expansion, and gradually decrease until reaching the surface of the model.

It can be seen that with the increasing of vertical displacement applied to the expansion damaged models, compressive force generated in the concrete model, and X shape cracking developed gradually until the failure of the structure is reached.

The internal stress reaction of ASR and DEF expanded concrete model is relatively close, but the maximum Compressive Strength and Elastic Modulus does show some of the differences.

And when considering free boundary condition loading, shown in Figure 1.10, the top and bottom of the concrete model can move freely in horizontal directions, thus the X-shape cracking pattern shown in fix boundary loading cases does now show up here.

As for the displacement change in each step, Compressive Strength is also recorded to show the residual mechanical properties of the expanded model. Besides, Elastic Modulus will also be calculated from the plotting of the load-displacement graph.

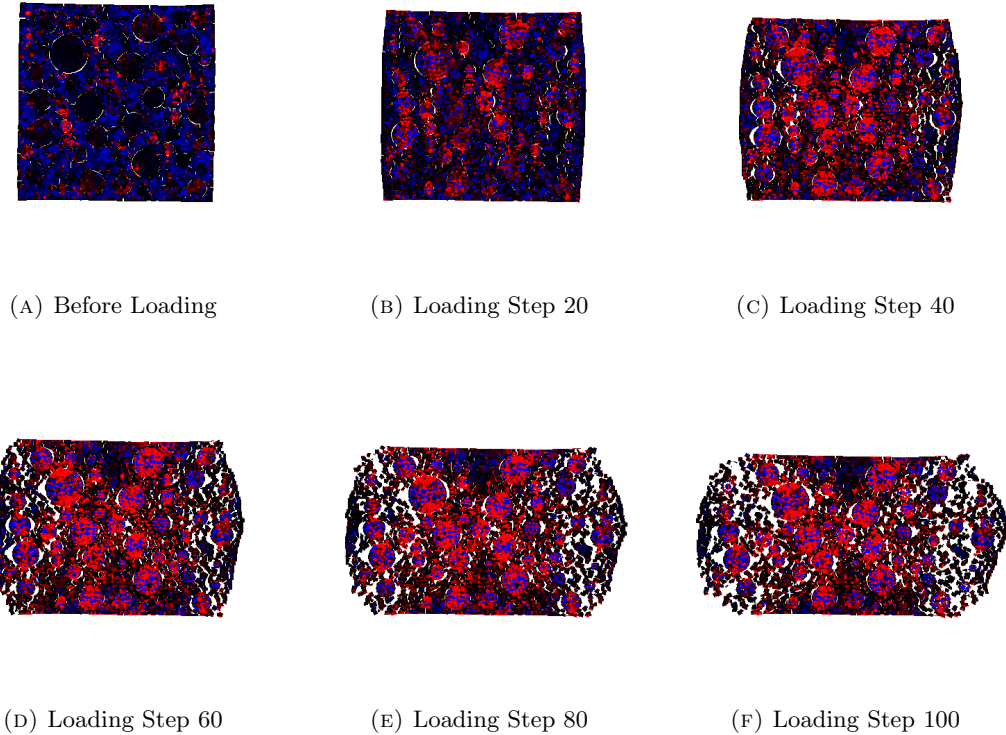


FIGURE 1.8: ASR Loading in Fixed Boundary Condition

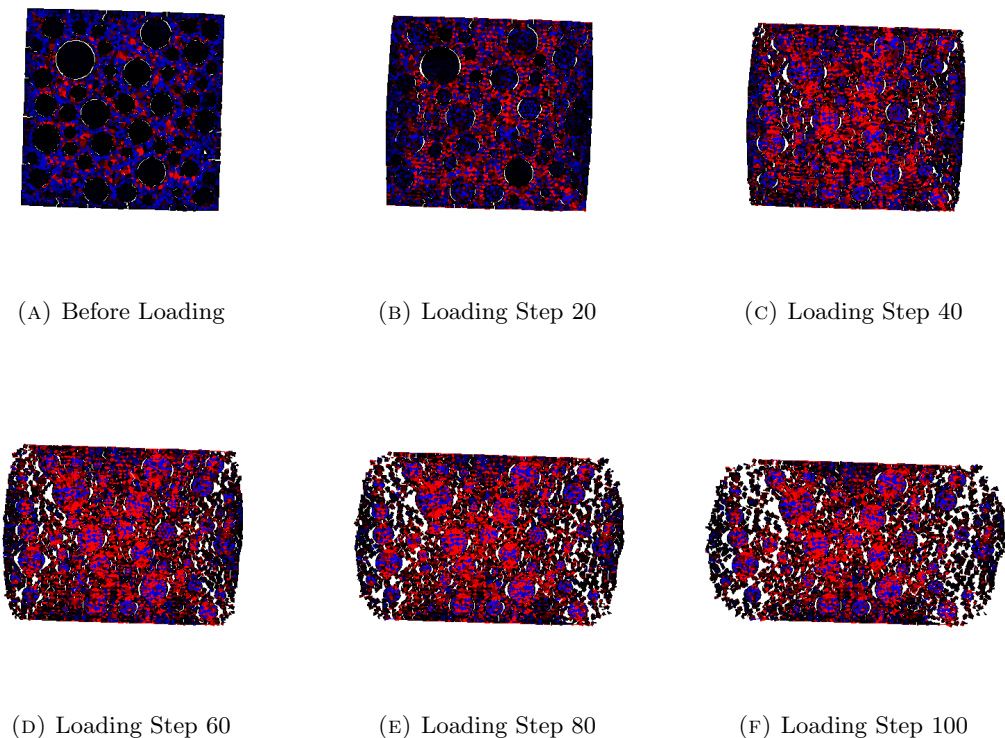


FIGURE 1.9: DEF Loading in Fixed Boundary Condition

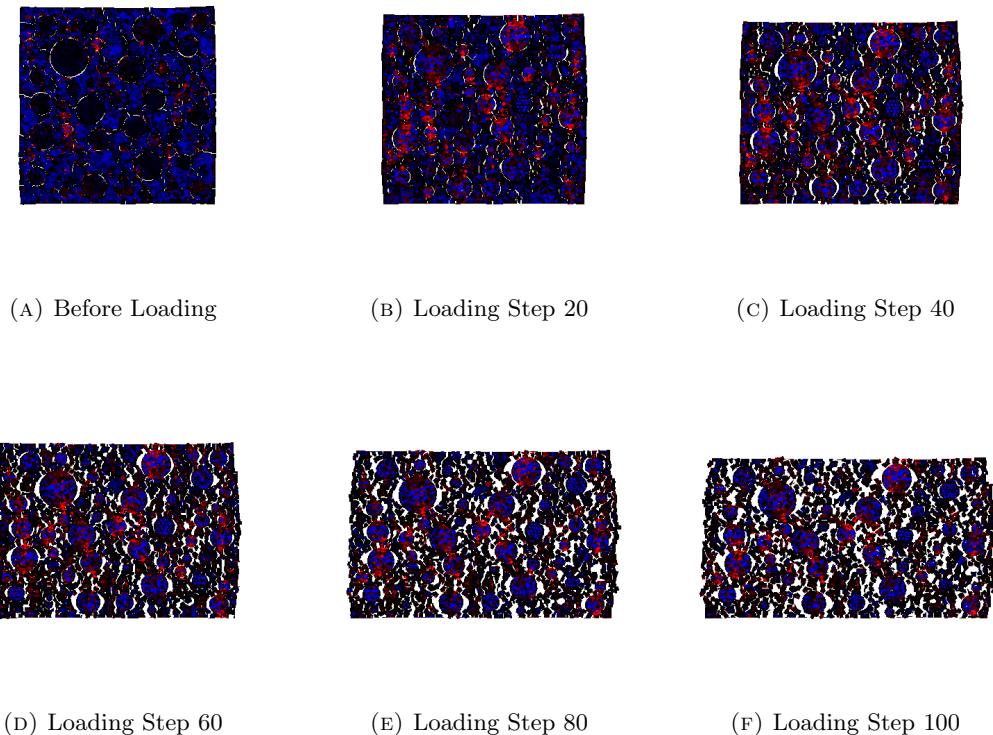


FIGURE 1.10: ASR Loading in Free Boundary Condition

1.3.1 Experimental Result of ASR Expansion on Mechanical Properties of Concrete

In first test study, Swamy and Asali[?] observed ASR-affected concrete in views of compressive strength, using 3 types Mixes (Control, 41/2% opal, 15% fused silica) for 1 year, in a cubic shape of size 100x100x100mm. The expansion is measured one-dimensionally.

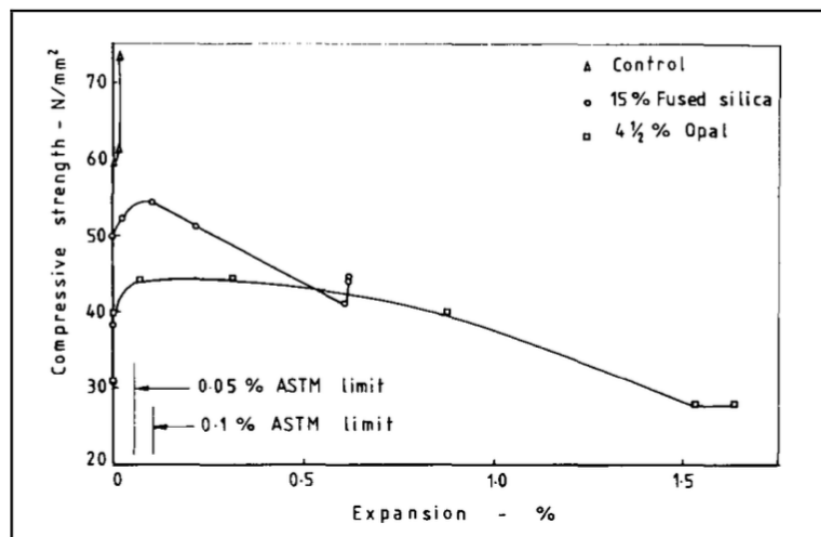
The results found are in Figure 1.11 as follow [Swamy & Al-Asali, 1988] .

Test	Mix	Age in days			
		10	28	100	365
Average Expansion (%)	Control	0.001	0.003	0.017	0.021
	4 ^{1/2} % Opal,	0.097	0.316	0.883	1.644
	15 % Fused Silica	0.005	0.023	0.259	0.623
Average Compressive Strength (N/mm²)	Control	--	60.1	61.9	73.5
	4 ^{1/2} % Opal,	--	44.5	39.9	27.5
	15 % Fused Silica	50.2	52.5	50.5	44.5

FIGURE 1.11: Effects of ASR expansion on compressive strength of concrete [Swamy & Al-Asali, 1988].

The compressive strength of opal concrete was 54% less than that the control concrete for 28 days, then reached to 63% at 1 year compared with the strength of control concrete. The loss in strength of fused silica concrete was nearly 26% at 28 days and 39% at 1 year as comparing it with that of control concrete [Swamy & Al-Asali, 1988].

In Figure 1.12, the loss in compressive strength of control concrete and ASR-affected concrete at different rates of expansion was shown, where drop of compressive strength of ASR-affected concretes becomes more clear with expansion [Swamy & Al-Asali, 1988].



Expansion, percent	4½ percent opal		15 percent fused silica	
	Age, days	Loss, percent	Age, days	Loss, percent
0.05	6	9	40	12
0.10	8	11	60	11
0.20	17	20	87	15
0.40	36	27	140	30
0.60	60	30	200	40
1.00	117	38	—	—
1.60	270	62	—	—

FIGURE 1.12: Loss of compressive strength of ASR-affected concrete with time [Swamy & Al-Asali, 1988]

T. Ahmed et al.[?] used Thames Valley sand (in Mix A), fused silica (in Mix B) and slowly reactive aggregate (in Mix C) to investigate the effect of ASR expansion on compressive strength of concrete, using specimens in size of 100x100x100 mm[BSEN 1290-3, 2000], cast and cured with respect to BS 1881 Part 122 [BS, 1881].

In this experiment, the cube specimens were cured for 28 days in water at 20°C and then the temperature was increased to 38°C to accelerate alkali-silica reaction. Then specimens were stored at water tank until 12 months passed [Ahmed et al., 2003]. After 28-days curing at 20°C and storage at 38°C for 12 months, the expansion ratios and compressive strength are given in Figure 1.13 [Ahmed et al., 2003].

Mix	A	B	C
Expansion ratio (mm/mm) for 28-days curing at 20 °C	-0.4	0.96	0.05
Compressive Strength (N/mm ²) for 28-days curing at 20 °C	50.3	41.0	46.8
Expansion ratio (mm/mm) for 12 months curing at 38 °C	4.3	16.86	1.27
Compressive Strength (N/mm ²) for 12 months curing at 38 °C	57.0	26.5	65.3

FIGURE 1.13: Effect of ASR expansion on compressive strength of concrete [Ahmed et al., 2003].

As seen in Figure 1.13, the results reveal that compressive strength of Mix A is nearly 7.5% higher than Mix C's (control mix) at 28 days due to no expansion in Mix A, while compressive strength of Mix A is nearly 12.7% less than Mix C's (control mix) at 12 months due to its greater expansion compared with expansion of Mix C. As for Mix B, which is with fused silica, the greatest expansion in the three mixes is achieved and compressive strength dropped nearly 12.4% for 28 days with compared to Mix C. After stored at hot water (38°C) for 12 months, the drop in strength of Mix B reached to nearly 59.4% [Ahmed et al., 2003].

Figure 3.1 reveals that a greater decrease in compressive strength was observed in Mix B compared with Mix A at any expansion percent due to different reaction rates for fused silica and Thames Valley sand permitting the hydration of cement to increase the compressive strength of concrete [Ahmed et al., 2003].

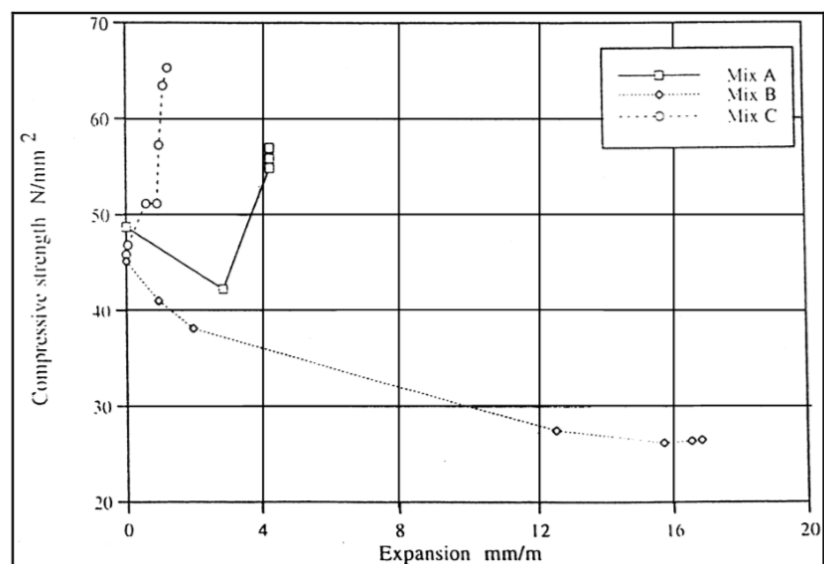


FIGURE 1.14: Change in compressive strength of ASR-affected concrete vs. time [Ahmed et al., 2003].

Giannini[?] carried out mechanical properties test on expanded specimens damaged by ASR and DEF expansion. Two sets of 4 x 8 in. (100 x 200 mm) cylinders were produced for the purpose of further evaluating the effects of ASR and DEF on the mechanical properties of concrete. This study expands on and complements the mechanical tests conducted on the core samples extracted from the exposure site specimens. Two reactive aggregates, Jobe (F1) sand and Placitas (C10) gravel were used, bringing the total number of reactive aggregates investigated in the overall project to four. A non-linear resonant frequency test method was also employed for selected test specimens. In this study, the cylinders are intended to represent a laboratory analog for core samples extracted from a field structure.

Here the experiment results for ASR expansion are presented. Figure 1.15 shows the compressive strength results for the Jobe (F1) and Placitas (C10) cylinders, respectively. Each data represents the average of three cylinders.

For the Jobe (F1) cylinders, decreases of 15% were measured. For the Placitas (C10) cylinders, an increase of 17% was measured for the ASR cylinders. The Placitas (C10) ASR cylinders expanded much more slowly than all other specimens in this study, and therefore were able to gain strength (possibly due to continued hydration of cement) more quickly than ASR could degrade it. However, the strength at 0.177% expansion (approximately 8 months of age) was almost 18% lower than that of the non-reactive control specimens at one year, so ASR did still have a negative impact on strength.

		Jobe (F1)						Placitas (C10)						
		Expansion Level (%)						Expansion Level (%)						
		0.009	0.109	0.181	0.272	0.379	0.416	0.429	0.010	0.045	0.074	0.135	0.160	0.177
E (GPa)*	Cyl 1	27.9	20.0	17.6	13.4	13.0	15.8	n/a	29.5	26.3	24.3	23.5	21.8	22.6
	Cyl 2	29.2	21.2	19.3	15.5	12.4	16.7	16.6	30.3	25.6	23.9	22.7	23.1	25.8
	Cyl 3	30.2	19.0	16.6	15.7	13.8	15.4	17.5	29.0	25.2	25.6	25.6	23.0	23.4
	Average	29.1	20.1	17.9	14.9	13.1	16.0	17.1	29.6	25.7	24.6	23.9	22.6	23.9
	Var %	7.9	11.0	15.2	15.4	11.3	7.8	5.3	4.5	4.3	7.2	12.1	5.7	13.4
f_c (MPa)*	Cyl 1	33.0	35.2	32.2	30.1	28.7	28.9	n/a	35.4	36.0	35.3	39.9	42.2	40.5
	Cyl 2	33.8	34.6	34.8	30.4	29.3	29.6	30.0	36.8	37.2	41.5	39.2	41.0	44.1
	Cyl 3	34.9	36.3	32.8	31.1	28.7	29.6	29.8	35.4	36.7	37.1	40.0	41.5	41.5
	Average	33.9	35.4	33.3	30.6	28.9	29.4	29.9	35.9	36.6	37.9	39.7	41.6	42.0
	Var %	5.4	4.6	7.9	3.3	2.1	2.3	0.7	3.9	3.2	16.4	1.9	2.9	8.6
E, % of predicted by f_c		105.6	71.3	65.4	56.9	51.3	62.3	66.0	104.5	89.7	84.5	80.1	74.1	78.0

* 1 GPa = 145 ksi; 1 MPa = 145 psi

FIGURE 1.15: Elastic modulus and compressive strength results for ASR cylinders[Giannini, 2012]

In study done by ALKANA (2014)[?], the effect of ASR expansion on mechanical properties of concrete and the effect of specimen types on ASR expansion were investigated. Mechanical tests were performed on both the specimens exceeding expansion from ASR of 0.04 percent and ones exceeding that of 0.10 percent.

In this part, the results for G-A concrete with greater than expansion of 0.04 percent, G-B concrete with greater than that of 0.10 percent, and G-C concrete (control concrete) were given with graphs and tables in the following parts. While ASR-affected concrete (G-A, G-B) were started to be stored at 60°C and 100% RH, G-B concrete was compulsorily exposed to NaOH solution in recent weeks in order to provide expansion percentage of G-B concrete to exceed the limit of 0.10 percent. G-C concrete, on the other hand, was cured in water at 20°C and used as control concrete. As known, the formed ASR gel absorbs water, expands, and causes internal pressure that causes cracking, which then continues and leads to expansion in concrete structure.

The ASR effect on compressive strength was examined by using cubic specimens, 150x150 mm in size, and cylindrical specimens, 100x200 mm in size. While the mix design of all specimens was prepared according to regulations as described by RILEM TC 219-ACS, compressive test for all specimens were carried out in accordance with the provisions in TS EN 12390-3. Limestone, non-reactive aggregate, and natural river sand, moderately reactive aggregate, were used as coarse and fine aggregates, respectively.

The expansion results in compressive strength for all specimens are given Figure 1.16, Figure 1.17 and Figure 1.18.

<u>G-A Concrete</u>		Age, weeks										at 60 °C and NaOH			
		Time elapsed at 60 °C and 100 % RH													
		2	3	4	6	8	10	12	14	15	16	17			
<u>Expansion %</u>	1	0.0163	0.0224	0.0343	0.0417	---	---	---	---	---	---	---	at 60 °C and NaOH		
	2	0.0165	0.0247	0.0337	0.0423	---	---	---	---	---	---	---			
	3	0.0173	0.0253	0.0345	0.0427	---	---	---	---	---	---	---			
	AV.	0.0167	0.0241	0.0342	0.0422	---	---	---	---	---	---	---			
<u>Compressive strength (MPa)</u>	AV.	---	---	---	48.5	---	---	---	---	---	---	---	---	---	---
<u>G-B Concrete</u>															
<u>Expansion %</u>	1	0.0175	0.0257	0.0337	0.0423	0.0497	0.0569	0.0594	0.0615	0.0789	0.0916	0.1006	at 60 °C and NaOH		
	2	0.0145	0.0233	0.0325	0.0425	0.0495	0.0566	0.0597	0.0622	0.0803	0.0920	0.1011			
	3	0.0163	0.0265	0.0367	0.0437	0.0513	0.0573	0.0604	0.0628	0.0806	0.0926	0.1013			
	AV.	0.0161	0.0252	0.0343	0.0428	0.0502	0.0569	0.0598	0.0622	0.0799	0.0921	0.1010			
<u>Compressive strength (MPa)</u>	AV.	---	---	---	---	---	---	---	---	---	---	45.1			
<u>G-C Concrete</u>		in water at 20 °C													
<u>Compressive strength (MPa)</u>	AV.	---	---	---	52.4	---	---	---	---	---	---	---	---	---	---

FIGURE 1.16: Expansion and compressive strength of all concretes for cube specimens[ALKANA, 2012]

<u>G-A Concrete</u>		Time elapsed at 60 °C and 100 % RH										at 60 °C and NaOH			
		Age, weeks													
		2	3	4	6	8	10	12	14	15	16	17	18		
<u>Expansion %</u>	1	0.0140	0.0215	0.0295	0.0370	0.0415	---	---	---	---	---	---	---		
	2	0.0150	0.0205	0.0280	0.0360	0.0400	---	---	---	---	---	---	---		
	3	0.0140	0.0215	0.0305	0.0350	0.0390	---	---	---	---	---	---	---		
	Av.	0.0143	0.0212	0.0293	0.0360	0.0402	---	---	---	---	---	---	---		
<u>Compressive strength (MPa)</u>	Av.	---	---	---	---	---	37.1	---	---	---	---	---	---		
<u>G-B Concrete</u>		in water at 20 °C													
<u>Expansion %</u>	1	0.0130	0.0210	0.0290	0.0360	0.0410	0.0455	0.0500	0.0525	0.0700	0.0850	0.0920	0.1025		
	2	0.0135	0.0195	0.0280	0.0350	0.0390	0.0435	0.0490	0.0505	0.0690	0.0810	0.0910	0.0990		
	3	0.0150	0.0185	0.0275	0.0335	0.0380	0.0430	0.0485	0.0505	0.0695	0.0795	0.0900	0.0990		
	Av.	0.0138	0.0197	0.0282	0.0348	0.0393	0.0440	0.0492	0.0512	0.0695	0.0818	0.0910	0.1002		
<u>Compressive strength (MPa)</u>	Av.	---	---	---	---	---	---	---	---	---	---	---	---	35.6	
<u>G-C Concrete</u>		in water at 20 °C													
<u>Compressive strength (MPa)</u>	Av.	---	---	---	---	---	40.7	---	---	---	---	---	---		

FIGURE 1.17: Expansion and compressive strength of all concretes for cylindrical specimens[ALKANA, 2012]

<u>Cube Specimens</u>		Age, weeks				
		Concrete	6	8	17	18
<u>Expansion %</u>	G-A	0.0422	---	---	---	---
	G-B	0.0428	0.0502	0.1010	---	---
<u>Compressive strength (MPa)</u>	G-A	48.5	---	---	---	---
	G-B	---	---	45.1	---	---
	G-C	52.4	---	---	---	---
<u>Loss in Compressive Strength (%)</u>	G-A	---	---	---	---	---
	G-B	7.6	---	14.1	---	---
<u>Cylindrical Specimens</u>						
<u>Expansion %</u>	G-A	0.0360	0.0402	---	---	---
	G-B	0.0348	0.0393	0.0910	0.1002	---
<u>Compressive strength (MPa)</u>	G-A	---	37.1	---	---	---
	G-B	---	---	---	35.6	---
	G-C	---	40.7	---	---	---
<u>Loss in Compressive Strength (%)</u>	G-A	---	8.9	---	---	---
	G-B	---	--	---	12.5	---

FIGURE 1.18: Loss in compressive strength of ASR-affected concrete comparing with control concrete [ALKANA, 2012]

1.3.2 Summary of Experimental Result of ASR Expansion on Mechanical Properties of Concrete

Reference	Type	Expansion (%)	Compressive Strength	Elastic Modulus	Speciment Dimension
Giannini (2012), Mixture 1	ASR	0.009	1.00	1.00	100 x 200 mm Cylinder
Giannini (2012), Mixture 1	ASR	0.109	1.04	0.69	100 x 200 mm Cylinder
Giannini (2012), Mixture 1	ASR	0.181	0.98	0.61	100 x 200 mm Cylinder
Giannini (2012), Mixture 1	ASR	0.272	0.90	0.51	100 x 200 mm Cylinder
Giannini (2012), Mixture 1	ASR	0.379	0.85	0.45	100 x 200 mm Cylinder
Giannini (2012), Mixture 1	ASR	0.416	0.87	0.55	100 x 200 mm Cylinder
Giannini (2012), Mixture 1	ASR	0.429	0.88	0.59	100 x 200 mm Cylinder
Giannini (2012), Mixture 2	ASR	0.01	1.00	1.00	100 x 200 mm Cylinder
Giannini (2012), Mixture 2	ASR	0.045	1.02	0.87	100 x 200 mm Cylinder
Giannini (2012), Mixture 2	ASR	0.074	1.06	0.83	100 x 200 mm Cylinder
Giannini (2012), Mixture 2	ASR	0.135	1.11	0.81	100 x 200 mm Cylinder
Giannini (2012), Mixture 2	ASR	0.16	1.16	0.77	100 x 200 mm Cylinder
Giannini (2012), Mixture 2	ASR	0.177	1.17	0.81	100 x 200 mm Cylinder

Reference	Type	Expansion (%)	Compressive Strength	Elastic Modulus	Speciment Dimension
ALKAN HAFCI (2013)	ASR	0.0422	0.93		150x150x150 mm Cube
ALKAN HAFCI (2013)	ASR	0.101	0.86		150x150x150 mm Cube
ALKAN HAFCI (2013)	ASR	0.0402	0.91		100 x 200 mm Cylinder
ALKAN HAFCI (2013)	ASR	0.1002	0.87		100 x 200 mm Cylinder
ALKAN HAFCI (2013)	ASR	0.0402		0.79	100 x 200 mm Cylinder
ALKAN HAFCI (2013)	ASR	0.1002		0.64	100 x 200 mm Cylinder

Reference	Type	Expansion (%)	Compressive Strength	Elastic Modulus	Speciment Dimension
T.Ahmed et al.(2003) Mix A	ASR	0	0.98	1.07	100x100x100 mm Cube
T.Ahmed et al.(2003) Mix A	ASR	0.27	0.83	0.99	100x100x100 mm Cube
T.Ahmed et al.(2003) Mix A	ASR	0.405	0.96	0.80	100x100x100 mm Cube
T.Ahmed et al.(2003) Mix A	ASR	0.405	0.71	0.43	100x100x100 mm Cube
T.Ahmed et al.(2003) Mix A	ASR	0.405	0.87	0.35	100x100x100 mm Cube
T.Ahmed et al.(2003) Mix B	ASR	0.02	0.74	0.27	100x100x100 mm Cube
T.Ahmed et al.(2003) Mix B	ASR	0.126	0.54	0.09	100x100x100 mm Cube
T.Ahmed et al.(2003) Mix B	ASR	0.156	0.46	0.09	100x100x100 mm Cube
T.Ahmed et al.(2003) Mix B	ASR	0.166	0.42	0.06	100x100x100 mm Cube
T.Ahmed et al.(2003) Mix B	ASR	0.17	0.41	0.05	100x100x100 mm Cube

Reference	Type	Expansion (%)	Compressive Strength	Elastic Modulus	Speciment Dimension
Swamy & Al-Asali (1988) 1 Mix 4.5%	ASR	0.316	0.74		100x100x100 mm Cube
Swamy & Al-Asali (1988) 1 Mix 4.5%	ASR	0.883	0.64		100x100x100 mm Cube
Swamy & Al-Asali (1988) 1 Mix 4.5%	ASR	1.644	0.37		100x100x100 mm Cube
Swamy & Al-Asali (1988) 1 Mix 4.5%	ASR	0.005	0.87		100x100x100 mm Cube
Swamy & Al-Asali (1988) 1 Mix 4.5%	ASR	0.023	0.82		100x100x100 mm Cube
Swamy & Al-Asali (1988) 1 Mix 4.5%	ASR	0.623	0.61		100x100x100 mm Cube
Swamy & Al-Asali (1988) 2 Mix 4.5%	ASR	0.05	0.91		100x100x100 mm Cube
Swamy & Al-Asali (1988) 2 Mix 4.5%	ASR	0.1	0.89		100x100x100 mm Cube
Swamy & Al-Asali (1988) 2 Mix 4.5%	ASR	0.2	0.80		100x100x100 mm Cube
Swamy & Al-Asali (1988) 2 Mix 4.5%	ASR	0.4	0.73		100x100x100 mm Cube
Swamy & Al-Asali (1988) 2 Mix 4.5%	ASR	0.6	0.70		100x100x100 mm Cube
Swamy & Al-Asali (1988) 2 Mix 4.5%	ASR	1	0.62		100x100x100 mm Cube
Swamy & Al-Asali (1988) 2 Mix 4.5%	ASR	1.6	0.38		100x100x100 mm Cube
Swamy & Al-Asali (1988) 2 Mix 4.5%	ASR	0.05	0.88		100x100x100 mm Cube
Swamy & Al-Asali (1988) 2 Mix 4.5%	ASR	0.1	0.89		100x100x100 mm Cube
Swamy & Al-Asali (1988) 2 Mix 4.5%	ASR	0.2	0.85		100x100x100 mm Cube
Swamy & Al-Asali (1988) 2 Mix 4.5%	ASR	0.4	0.70		100x100x100 mm Cube
Swamy & Al-Asali (1988) 2 Mix 4.5%	ASR	0.6	0.60		100x100x100 mm Cube

Reference	Type	Expansion (%)	Compressive Strength	Elastic Modulus	Speciment Dimension
Swamy & Al-Asali (1988) 3 Mix 4.5%	ASR	0.004		0.97	100x100x100 mm Cube
Swamy & Al-Asali (1988) 3 Mix 4.5%	ASR	0.071		0.80	100x100x100 mm Cube
Swamy & Al-Asali (1988) 3 Mix 4.5%	ASR	0.097		0.58	100x100x100 mm Cube
Swamy & Al-Asali (1988) 3 Mix 4.5%	ASR	0.316		0.49	100x100x100 mm Cube
Swamy & Al-Asali (1988) 3 Mix 4.5%	ASR	0.883		0.44	100x100x100 mm Cube
Swamy & Al-Asali (1988) 3 Mix 4.5%	ASR	1.644		0.23	100x100x100 mm Cube
Swamy & Al-Asali (1988) 3 Mix 4.5%	ASR	0.005		0.98	100x100x100 mm Cube
Swamy & Al-Asali (1988) 3 Mix 4.5%	ASR	0.023		0.96	100x100x100 mm Cube
Swamy & Al-Asali (1988) 3 Mix 4.5%	ASR	0.259		0.54	100x100x100 mm Cube
Swamy & Al-Asali (1988) 3 Mix 4.5%	ASR	0.623		0.42	100x100x100 mm Cube
Swamy & Al-Asali (1988) 4 Mix 4.5%	ASR	0		0.95	100x100x100 mm Cube
Swamy & Al-Asali (1988) 4 Mix 4.5%	ASR	0.071		0.80	100x100x100 mm Cube
Swamy & Al-Asali (1988) 4 Mix 4.5%	ASR	0.097		0.58	100x100x100 mm Cube
Swamy & Al-Asali (1988) 4 Mix 4.5%	ASR	0.316		0.49	100x100x100 mm Cube
Swamy & Al-Asali (1988) 4 Mix 4.5%	ASR	0.883		0.44	100x100x100 mm Cube
Swamy & Al-Asali (1988) 4 Mix 4.5%	ASR	1.442		0.25	100x100x100 mm Cube
Swamy & Al-Asali (1988) 4 Mix 4.5%	ASR	1.618		0.18	100x100x100 mm Cube
Swamy & Al-Asali (1988) 4 Mix 4.5%	ASR	1.644		0.23	100x100x100 mm Cube
Swamy & Al-Asali (1988) 4 Mix 4.5%	ASR	0		0.97	100x100x100 mm Cube
Swamy & Al-Asali (1988) 4 Mix 4.5%	ASR	0		0.96	100x100x100 mm Cube
Swamy & Al-Asali (1988) 4 Mix 4.5%	ASR	0.005		0.98	100x100x100 mm Cube
Swamy & Al-Asali (1988) 4 Mix 4.5%	ASR	0.023		0.96	100x100x100 mm Cube
Swamy & Al-Asali (1988) 4 Mix 4.5%	ASR	0.259		0.54	100x100x100 mm Cube
Swamy & Al-Asali (1988) 4 Mix 4.5%	ASR	0.615		0.32	100x100x100 mm Cube
Swamy & Al-Asali (1988) 4 Mix 4.5%	ASR	0.625		0.40	100x100x100 mm Cube
Swamy & Al-Asali (1988) 4 Mix 4.5%	ASR	0.623		0.42	100x100x100 mm Cube

1.3.3 Experimental Result of DEF Expansion on Mechanical Properties of Concrete

In first test study, Bruetaud et al.[?] observed DEF-affected concrete in views of compressive strength. Figure 1.19 summarizes the mix designs of these different concretes.

Mix designs of the concrete, unit: Kg/m³

	Siliceous aggregates		Calcareous aggregates		W/ C=0.48	W/ C=0.35
	W/ C=0.48	W/ C=0.35				
<i>Particle size [mm]</i>						
0/0.315	183	192				
0.315/1	134	141	Dry sand (S)		711	769
1/4	217	228				
2/4	232	244				
4/8	180	189	Dry gravels (G)		1067	1154
8/12.5	842	885				
Water reducer: 0.6%	/	2,52	Water reducer: 0.6%		/	2.63
KOH to 0.75%	1.52	1.60	KOH to 0.75%		1.54	1.66
KOH to 1.00%	3.04	3.19	/			
Water (W)	192	146	Water (W)		199	159
Cement (C)	400	420	Cement (C)		405	438

FIGURE 1.19: Mix designs of the concrete, DEF cylinders[Bruetaud et al., 2008]

Each concrete sample was cast and cured in 3 cylindrical moulds whose dimensions are 11 cm (diameter) and 22 cm (height) to generate 3 identical concrete specimens. The moulds were covered so as to limit water exchange. The applied heat treatment followed a cycle divided into four different steps, as shown in Figure 1.20. Some concrete samples were not heat treated but were conventionally cured at 20 °C to be used as reference. After the heat treatment, samples were stored at 20 °C in 100% relative humidity until 28 days. Next, wetting and drying cycles were applied in accordance with LPC no. 59 pre-test method, to increase the kinetics of DEF reaction without changing its triggering conditions. Samples are subjected to 2 cycles, each one lasting 14 days. A cycle consists of 7 days of drying at 38 °C and 30% relative humidity followed by 7 days of immersion in tap water at 20 °C. The volume of water with respect to the volume of the sample is kept under 1.5 to limit leaching effects. Once the cycles are finished, samples are stored into 3 individual hermetic boxes (to avoid carbonation) whose dimensions barely exceed those of the sample, to minimize the amount of water required for their immersion.[Bruetaud et al., 2008]

During this last period, expansion measurements were performed with an extensometer whose resulting measurement dispersion on the basis of three concrete specimens is less than 0.002%.

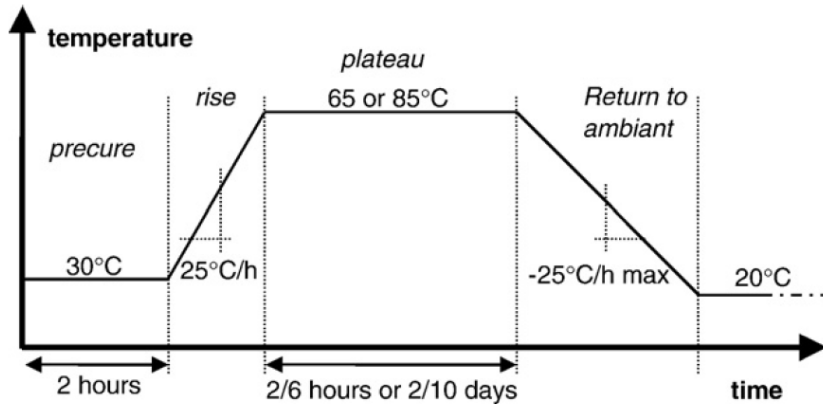


FIGURE 1.20: Heat treatment phases of DEF cylinders[Bruetaud et al., 2008]

In the case of 0.48-Si concretes (“heating” experiments), a relationship can be obtained between the ultimate compressive strength (residual strength) and the final expansion achieved. Typically, the strength of unaffected 0.48-Si concrete specimens reaches about 40 MPa. The most damaged specimens of 0.48-Si concretes fall down to 15 MPa, which represents a very significant decrease.[Bruetaud et al., 2008]

In Figure 1.21, the linear approximation would forecast a fall of strength on the order of 90% for a 1.6% expansion. This value, certainly exaggerated by the linear approximation, serves to verify that high expansion (over 1%) leads to very low residual mechanical strength. The linear approximation proposed in Figure 1.21 seems to imply that a DEF-related expansion lower than 0.20% will not generate significant loss in compressive strength.[Bruetaud et al., 2008]

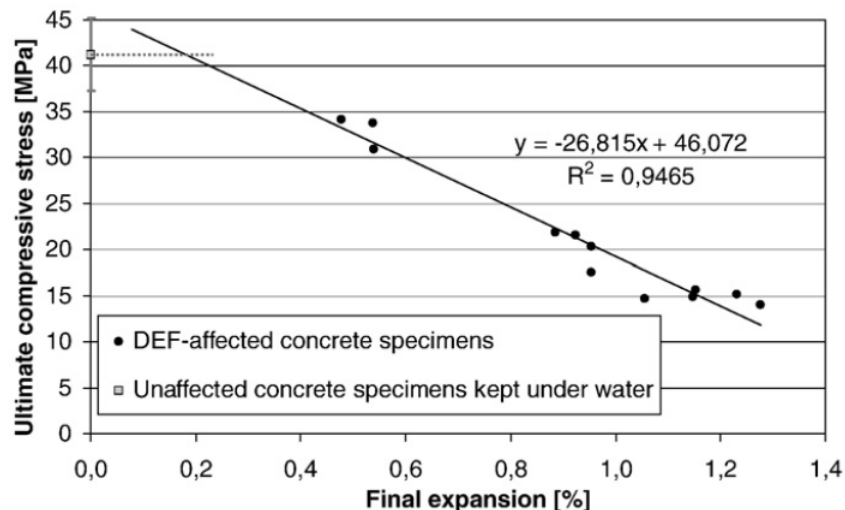


FIGURE 1.21: Compressive stress versus final expansion for the concrete specimens of the heating design of experiments[Bruetaud et al., 2008]

Together with ASR expansion, Giannini[?] also carried out mechanical properties test on expanded specimens damaged by DEF expansion.

Similar two sets of 4 x 8 in. (100 x 200 mm) cylinders were produced for the purpose of further evaluating the mechanical properties of damaged concrete. Two types of aggregates, Jobe (F1) sand and Placitas (C10) gravel were used. A non-linear resonant frequency test method was also employed for selected test specimens. The cylinders are intended to represent a laboratory analog for core samples extracted from a field structure.

Here the experiment results for DEF expansion are presented. Figure 1.22 shows the compressive strength results for the Jobe (F1) and Placitas (C10) cylinders, respectively. Each data represents the average of three cylinders. For the Jobe (F1) cylinders, decreases of 41% were measured. For the Placitas (C10) cylinders, a decrease of 24% is measured.[Giannini, 2012]

		Jobe (F1)						Placitas (C10)						
		Expansion Level (%)						Expansion Level (%)						
		0.000	0.102	0.208	0.344	0.415	0.506	1.011	0.008	0.079	0.179	0.266	0.327	0.454
1st Cycle Area (Pa)*	Cyl 1	324	494	917	3850	3699	5655	5399	435	1034	1592	1892	1363	3348
	Cyl 2	507	720	2576	3311	6598	5265	9375	177	807	1268	1800	775	3346
	Cyl 3	576	1327	2058	4971	3904	5367	5495	714	1216	1015	1359	1705	2942
	Average	469	847	1850	4044	4734	5429	6756	442	1019	1292	1684	1281	3212
	Var %	53.7	98.3	89.7	41.0	61.2	7.2	58.8	121.5	40.1	44.7	31.7	72.6	12.6
Plastic Strain ($\mu\epsilon$)	Cyl 1	27	69	91	557	494	878	787	52	140	145	206	214	616
	Cyl 2	88	104	364	479	1122	793	1569	n/a	108	145	253	109	421
	Cyl 3	79	160	253	747	602	821	826	103	179	86	153	179	347
	Average	65	111	236	594	739	830	1060	78	142	125	204	167	462
	Var %	95.6	81.8	115.9	45.0	85.0	10.2	73.7	65.8	50.1	47.3	49.3	62.9	58.2
f'_c (28 day)		29.8						33.9						
Load, % of 28-day f'_c		33.6						29.5						
Load, % of f'_c at test		36.6	35.2	38.1	50.9	53.4	54.5	62.7	30.3	30.4	30.8	34.1	30.4	39.7

* 1 Pa = 0.000145 psi; 1 MPa = 145 psi

FIGURE 1.22: Elastic modulus and compressive strength results for DEF cylinders[Giannini, 2012]

In experiments performed by Bouzabata et al.[?], DEF expansion for restrained and stress free on mortar prisms (40x40x160 mm) were presented. The water/cement ratio was 0.55 and the sand/cement ratio was 3. The chemical composition of the Portland cement used is given in Figure 1.23. As in the previous experiments, 3.1% of Na_2SO_4 was added to the mixing water. Siliceous sand known to be non-alkali-reactive was used.

Chemical compositions of cement and aggregate (%).

	SiO ₂	Al ₂ O ₃	Fe ₂ O ₃	CaO	MgO	SO ₃	K ₂ O	Na ₂ O	Na ₂ Oeq	Loi
Cement	19.3	4.6	2.2	63.9	2.4	3.3	1.1	0.3	1.02	-
Aggregate	96.1	-	0.4	1.38	0.24	-	0.72	0.79	1.26	0.4

FIGURE 1.23: Chemical compositions of cement and aggregate (%) mortar prisms [Bouzabata et al., 2012]

After casting, some of the specimens were cured at high temperatures with the heat treatment: 1 h at 20 °C, an increase from 20 to 80 °C in 4 h, a constant temperature of 80 °C for 10 h then a cooling to 20 °C in 10 h. The specimens were steamed in metal moulds, wrapped in watertight plastic film and covered by a metal plate to prevent evaporation of water during the heat treatment. At the same time, other specimens made in the same batch were stored at 20 °C. After cooling and demoulding, specimens were kept at 20 °C in endogenous conditions (sealed in plastic bags) for 28 days. [Bouzabata et al., (2012)]

Strains of specimens kept immersed in water after 28 days in stress-free conditions have been plotted in Figure 1.24. The specimens that had been subjected to the heat treatment during the curing period showed large expansions of between 1.3 and 2.2% due to DEF. All the specimens in stress-free conditions exhibited mapcracking. The first significant cracks appeared for a strain of about 0.5% (after 80 days of immersion in water). Compressive strength was measured on prismatic specimens (40x40x40mm) at time-steps chosen according to the expansions measured on the specimens (Figure 1.24).[Bouzabata et al., (2012)]

The evolution of the compressive strength of the reference mortar and of the mortar damaged by delayed ettringite formation have been plotted in Figure 1.25. The reference specimens showed the usual increase of compressive strength with time due to continuous cement hydration. The specimens that had been subjected to the heat treatment showed a decrease in strength around 40%. A large strength decrease occurred mainly between 70 and 100 days, corresponding to the significant increase of expansion, and the compressive strength reached a minimum value of 25MPa at 180 days.[Bouzabata et al., (2012)]

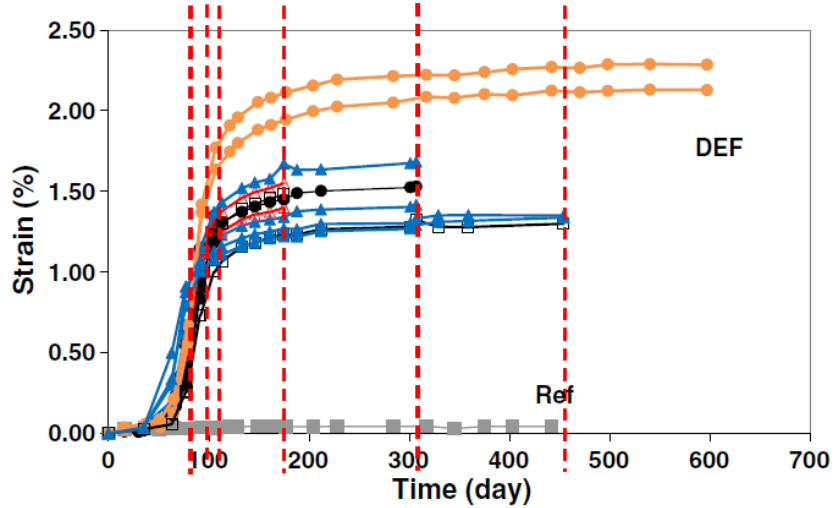


FIGURE 1.24: Strain of specimens in stress-free conditions (each line corresponds to one specimen, specimens of a same batch are plotted with the same marker — dotted lines show the times of the mechanical tests). [Bouzabata et al., (2012)]

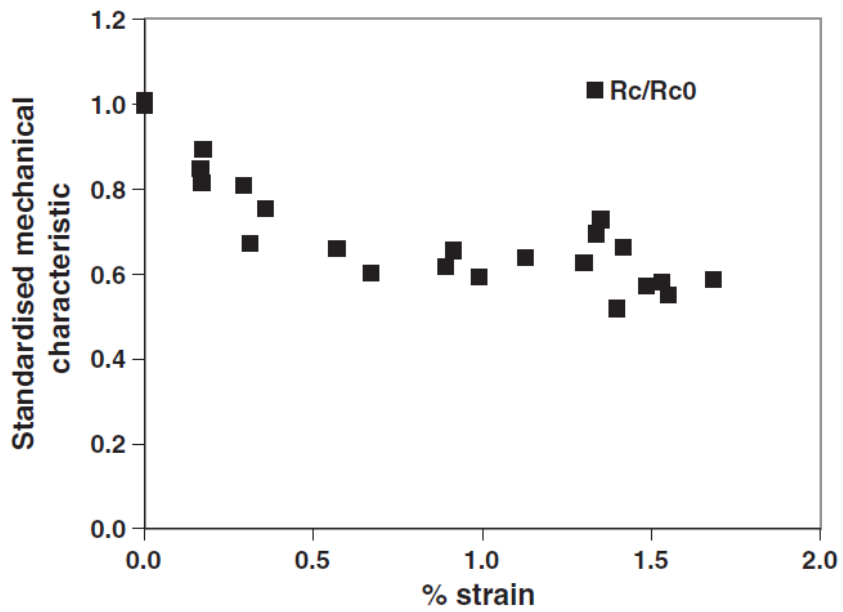


FIGURE 1.25: Decrease of compressive strength according to DEF expansion [Bouzabata et al., 2012]

Figure 2 summarizes the mix design of the concrete used in the construction of the raft foundation, done by M. Al Shamaa et al., 2014 [?]. Concrete is made with calcareous aggregates (in order to avoid the risk of alkali-aggregate reaction) and Portland cement CEM II/A-LL 42.5 R, which can be susceptible to an expansive behavior due to DEF. Concrete specimens were prepared according to the standards NF P 18-400 and NF P 18-422. Samples were cast in cylindrical molds whose dimensions are 11 cm (diameter) and 22 cm (height).

After casting, a part of concrete specimens was cured under heat treatments, shown in Figure 1.26. The maximum temperature in cycle reached maximum 70°C to expose concrete to a more severe condition by taking into account the variability of the properties of the material. Then the duration of the heat treatment was 18 days.

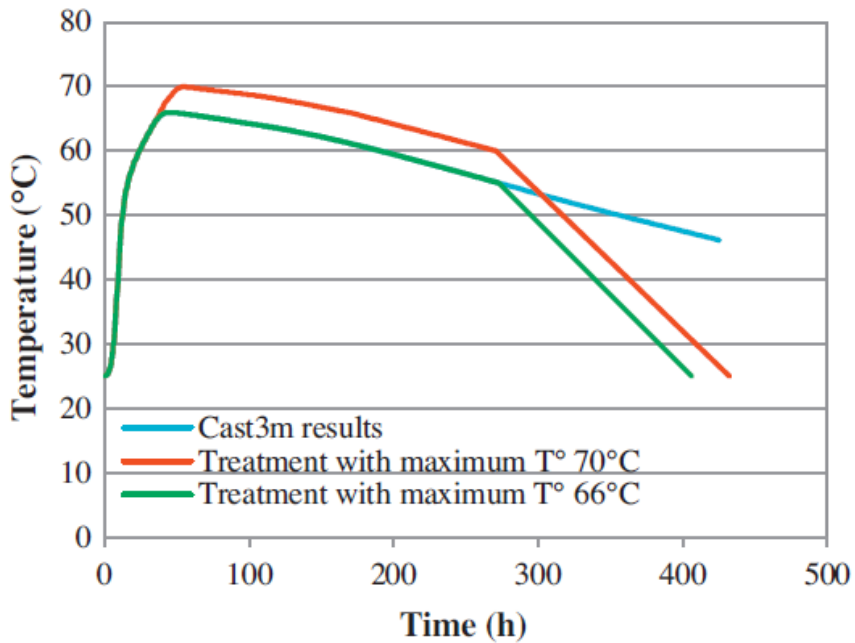


FIGURE 1.26: Experimental applied heat treatments [M. Al Shamaa et al., 2014]

Figure 1.27 shows a comparison of compressive strength and Young's modulus at the age of 28 days for different concretes.

Due to heat treatments, a decrease appeared of approximately 20% of the compressive strength. This decrease was observed in both concretes T70-Im and T66-Im. Thus, the application of heat curing induces a lower value of mechanical resistance before the concrete is affected by DEF.

However, the Young's modulus does not seem to be affected by the heat treatment. On the other hand, Figure 1.28 shows that the concrete T70-Im, which suffers from DEF, presents a degradation of its mechanical properties. We observe a 23% reduction in the compressive strength when the expansion was evolved from 0.08% at the age of 180 days

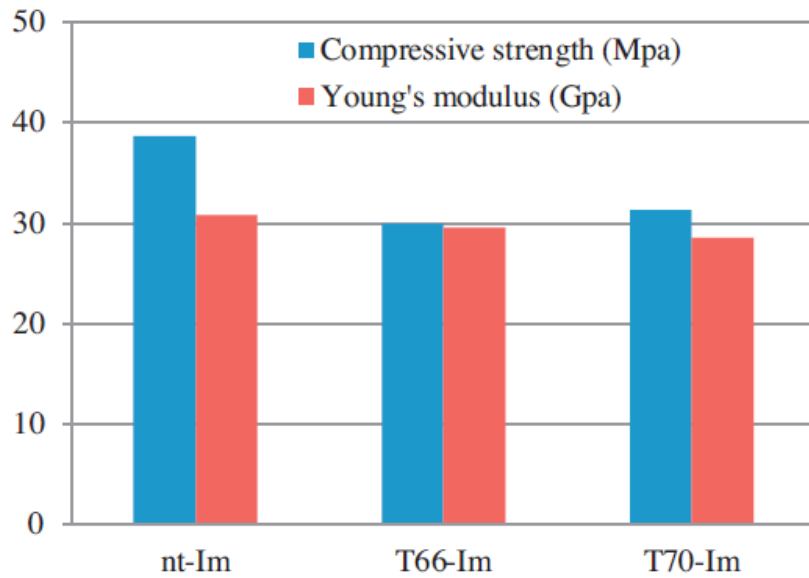


FIGURE 1.27: Effect of heat treatment on the compressive strength and Young's modulus at 28 days. [M. Al Shamaa et al., 2014]

to 0.20% at the age of 390 days. This loss is also observed for the Young's modulus and may be an indicator of the damage of the material.

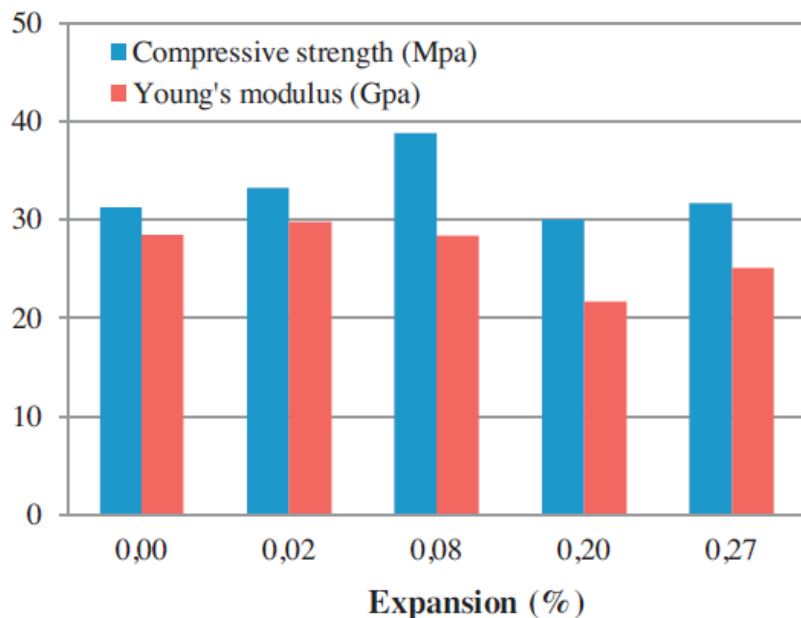


FIGURE 1.28: Relationship between the compressive strength, the Young's modulus and the expansion for concrete T70-Im. [M. Al Shamaa et al., 2014]

However, the strength loss is not proportional to the expansion reached. In fact, we observe, according to our last measurements (at the age of 640 days when the expansion reaches 0.27%), that the concrete tends to regain a part of its mechanical performance

he had lost. This delayed re-increase is observed both on the compressive strength, the dynamic and the Young's modulus.

These quantities have a minimum. Minima are observed at around 400 days when the inflection point of the slowdown in the expansion curve is reached Figure 1.30. On the other hand, all measurements on the concrete T66-Im concern only small expansions and the mechanical performances of this concrete was not affected until now (Figure ??).

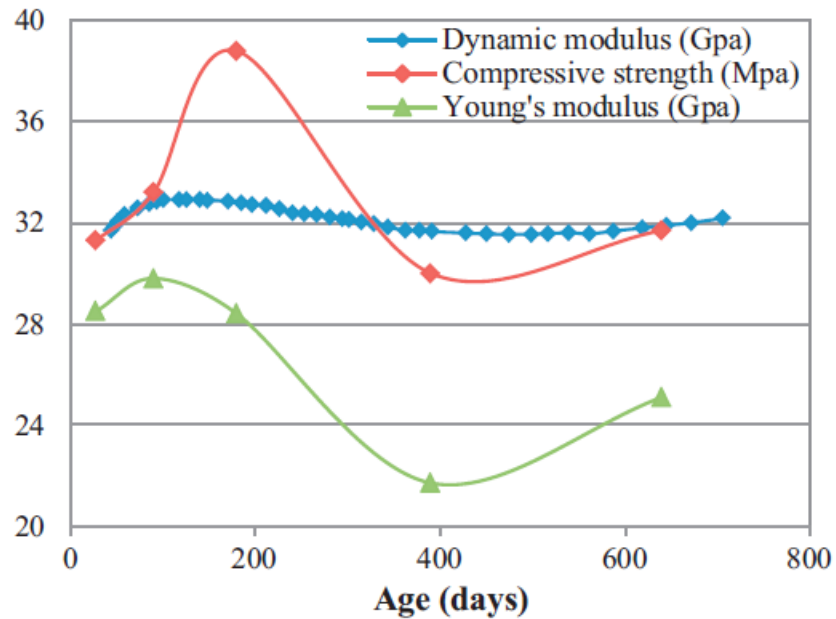


FIGURE 1.29: Mechanical properties versus time for concrete T70-Im. [M. Al Shamaa et al., 2014]

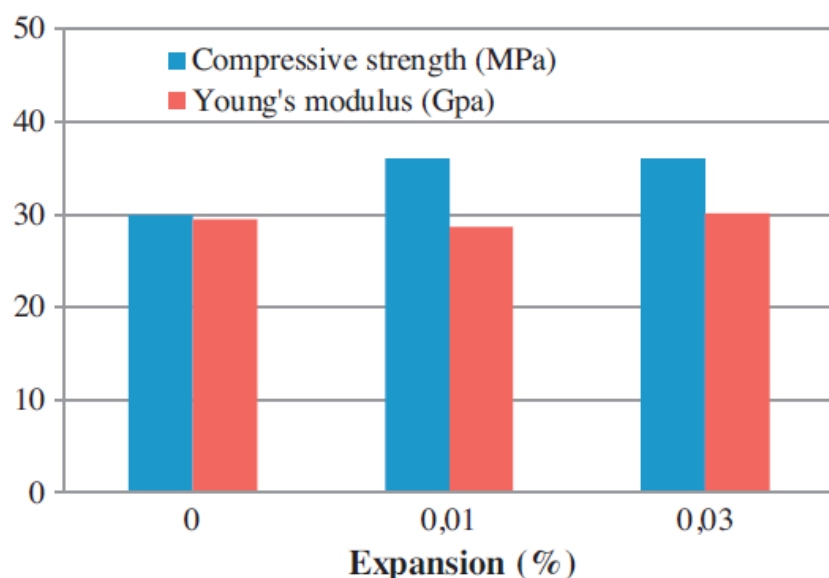


FIGURE 1.30: Relationship between the compressive strength, the Young's modulus and the expansion for concrete T66-Im. [M. Al Shamaa et al., 2014]

1.3.4 Summary of Experimental Result of DEF Expansion on Mechanical Properties of Concrete

Reference	Type	Expansion (%)	Compressive Strength Remained	Elastic Modulus Remained	Speciment Dimension
Giannini (2012), Mixture 1	DEF	0	1.00	1.00	100 x 200 mm Cylinder
Giannini (2012), Mixture 1	DEF	0.102	1.04	0.87	100 x 200 mm Cylinder
Giannini (2012), Mixture 1	DEF	0.208	0.96	0.64	100 x 200 mm Cylinder
Giannini (2012), Mixture 1	DEF	0.344	0.72	0.35	100 x 200 mm Cylinder
Giannini (2012), Mixture 1	DEF	0.415	0.69	0.33	100 x 200 mm Cylinder
Giannini (2012), Mixture 1	DEF	0.506	0.67	0.29	100 x 200 mm Cylinder
Giannini (2012), Mixture 1	DEF	1.011	0.58	0.25	100 x 200 mm Cylinder
Giannini (2012), Mixture 2	DEF	0.008	1.00	1.00	100 x 200 mm Cylinder
Giannini (2012), Mixture 2	DEF	0.079	1.00	0.85	100 x 200 mm Cylinder
Giannini (2012), Mixture 2	DEF	0.179	0.98	0.76	100 x 200 mm Cylinder
Giannini (2012), Mixture 2	DEF	0.266	0.89	0.69	100 x 200 mm Cylinder
Giannini (2012), Mixture 2	DEF	0.327	1.00	0.79	100 x 200 mm Cylinder
Giannini (2012), Mixture 2	DEF	0.454	0.76	0.41	100 x 200 mm Cylinder

Reference	Type	Expansion (%)	Compressive Strength Remained	Elastic Modulus Remained	Speciment Dimension
Brunetaud et al. (2008)	DEF	0	1.00		110 x 220 mm Cylinder
Brunetaud et al. (2008)	DEF	0.477631579	0.83		110 x 220 mm Cylinder
Brunetaud et al. (2008)	DEF	0.540789474	0.82		110 x 220 mm Cylinder
Brunetaud et al. (2008)	DEF	0.538157895	0.75		110 x 220 mm Cylinder
Brunetaud et al. (2008)	DEF	0.888157895	0.53		110 x 220 mm Cylinder
Brunetaud et al. (2008)	DEF	0.926315789	0.52		110 x 220 mm Cylinder
Brunetaud et al. (2008)	DEF	0.955263158	0.50		110 x 220 mm Cylinder
Brunetaud et al. (2008)	DEF	0.956578947	0.43		110 x 220 mm Cylinder
Brunetaud et al. (2008)	DEF	1.059210526	0.36		110 x 220 mm Cylinder
Brunetaud et al. (2008)	DEF	1.148684211	0.36		110 x 220 mm Cylinder
Brunetaud et al. (2008)	DEF	1.153947368	0.38		110 x 220 mm Cylinder
Brunetaud et al. (2008)	DEF	1.231578947	0.37		110 x 220 mm Cylinder
Brunetaud et al. (2008)	DEF	1.280263158	0.34		110 x 220 mm Cylinder

Reference	Type	Expansion (%)	Compressive Strength Remained	Elastic Modulus Remained	Speciment Dimension
Bouzabata et al. (2012)	DEF	0.004700353		1.02	40x40x160 mm Prism
Bouzabata et al. (2012)	DEF	0.002350176		1.00	40x40x160 mm Prism
Bouzabata et al. (2012)	DEF	0.173913043		0.90	40x40x160 mm Prism
Bouzabata et al. (2012)	DEF	0.166862515		0.85	40x40x160 mm Prism
Bouzabata et al. (2012)	DEF	0.178613396		0.81	40x40x160 mm Prism
Bouzabata et al. (2012)	DEF	0.291421857		0.81	40x40x160 mm Prism
Bouzabata et al. (2012)	DEF	0.361927145		0.76	40x40x160 mm Prism
Bouzabata et al. (2012)	DEF	0.314923619		0.68	40x40x160 mm Prism
Bouzabata et al. (2012)	DEF	0.568742656		0.66	40x40x160 mm Prism
Bouzabata et al. (2012)	DEF	0.665099882		0.61	40x40x160 mm Prism
Bouzabata et al. (2012)	DEF	0.897767333		0.62	40x40x160 mm Prism
Bouzabata et al. (2012)	DEF	0.918918919		0.65	40x40x160 mm Prism
Bouzabata et al. (2012)	DEF	0.982373678		0.59	40x40x160 mm Prism
Bouzabata et al. (2012)	DEF	1.130434783		0.64	40x40x160 mm Prism
Bouzabata et al. (2012)	DEF	1.318448884		0.62	40x40x160 mm Prism
Bouzabata et al. (2012)	DEF	1.346650999		0.68	40x40x160 mm Prism
Bouzabata et al. (2012)	DEF	1.35840188		0.73	40x40x160 mm Prism
Bouzabata et al. (2012)	DEF	1.403055229		0.52	40x40x160 mm Prism
Bouzabata et al. (2012)	DEF	1.424206816		0.67	40x40x160 mm Prism
Bouzabata et al. (2012)	DEF	1.485311398		0.57	40x40x160 mm Prism
Bouzabata et al. (2012)	DEF	1.539365452		0.59	40x40x160 mm Prism
Bouzabata et al. (2012)	DEF	1.555816686		0.55	40x40x160 mm Prism
Bouzabata et al. (2012)	DEF	1.689776733		0.58	40x40x160 mm Prism

Reference	Type	Expansion (%)	Compressive Strength Remained	Elastic Modulus Remained	Speciment Dimension
Al Shamaa et al. (2014)	DEF	0	1.00	1.00	110 x 220 mm Cylinder
Al Shamaa et al. (2014)	DEF	0.02	1.06	1.04	110 x 220 mm Cylinder
Al Shamaa et al. (2014)	DEF	0.08	1.25	1.00	110 x 220 mm Cylinder
Al Shamaa et al. (2014)	DEF	0.2	0.97	0.76	110 x 220 mm Cylinder

1.3.5 Residual Capabilities after Pure ASR Expansion

Here the uni-axial compression test result for ASR expanded concrete model is summarised.

As an example, compression test for cases with 30% coarse aggregate, of which 75% are set to be ASR reactive, will be presented in details.

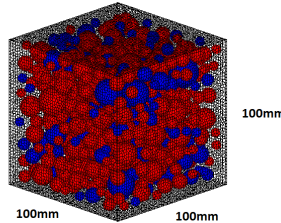


FIGURE 1.31: 30% Coarse Aggregate

As introduced previously in chapter 2 and chapter 3, one-dimensional global expansion up to 1.3% has been achieved by giving initial strain step by step at the interfaces between reactive aggregate and paste elements.

After expansion, three-dimensional expanded concrete models are tested under uni-axial compression condition. Displacement of loading boundary is controlled, as the top boundary of the concrete model moves downwards 0.02mm in each step. Top and bottom boundaries are under fix condition.

In each step of loading, compressive strength in the current step is recorded. As shown in Figure 1.32, the Load-Displacement curve obtained here is close to the shape of the normal concrete under fixed boundary compressive test, with increasing strength until reaching the maximum compressive strength, then decreasing until failure happens.

Also, in Figure 1.32, the trend of decreasing in maximum compressive strength along with the increasing of one-dimensional global expansion is also shown. With the global expansion increasing up to 1.3%, the compressive strength reduced gradually to 15.993MPa, which is 53% of undamaged model.

The Elastic Modulus, which here calculated as the maximum slope before compressive strength reaching the maximum, also shows the same trend when global expansion increase. While the Elastic Modulus is 33.8GPa for undamaged model, Elastic Modulus drop to 1.11GPa when global expansion reached 1.3%.

Loading with free boundary condition is also simulated here, and presented in Figure 1.33. As the boundary are set to be without horizontal frictions, cracks are more easier to open during loading, result in a generally 30% smaller compressive strength comparing

to the result from fixed boundary loading test. This is also corroborating with cases in reality. A similar decreasing trend in compressive strength and elastic modulus along with the increase of global expanding ratio can be obtained.

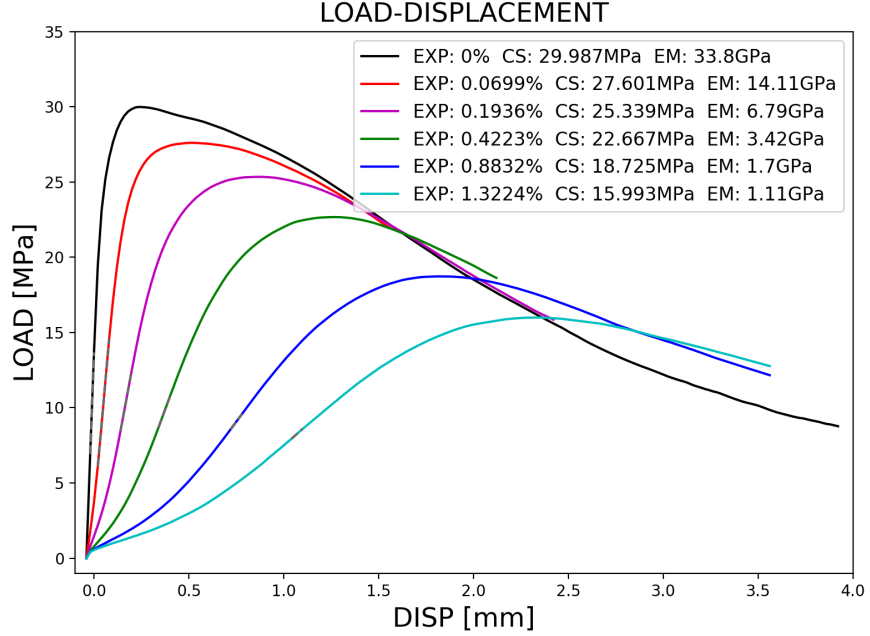


FIGURE 1.32: A30 P75 Fix Load-Displacement

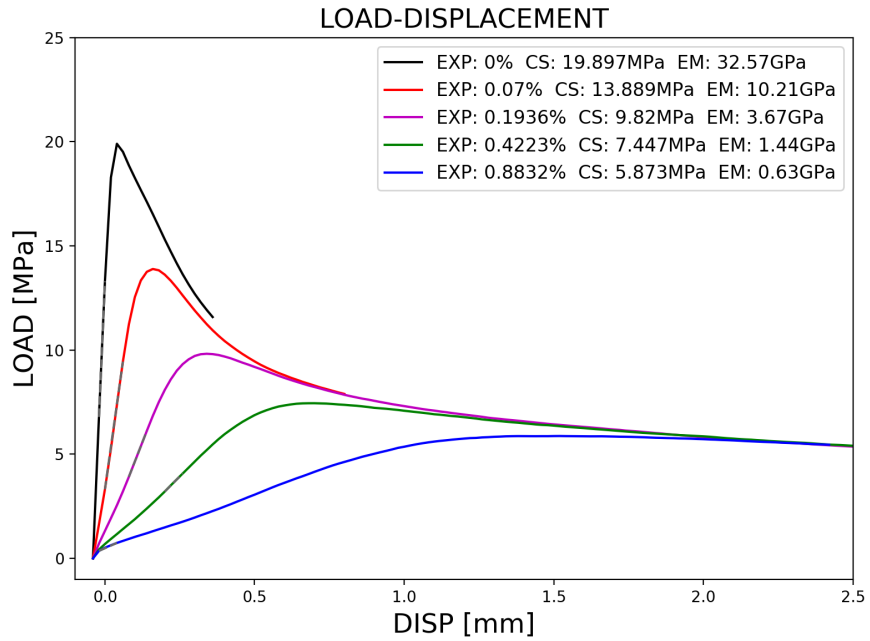


FIGURE 1.33: A30 P75 Free Load-Displacement

Here if plot the Residual Compressive Strength obtained from fixed boundary expansion with the one dimensional global expansion, it can be seen that the trend is quite close

with some of the experimental results, especially the results from Swamy & Al-Asali, 1988 (Figure ??)[?].

The trend of lossing in residual compressive strength along with the increasing in expansion is well presented. Though the model used in this simulation is not identical with the experimental one, it does show similar trend in relatively ratio of residential compressive strength lossing.

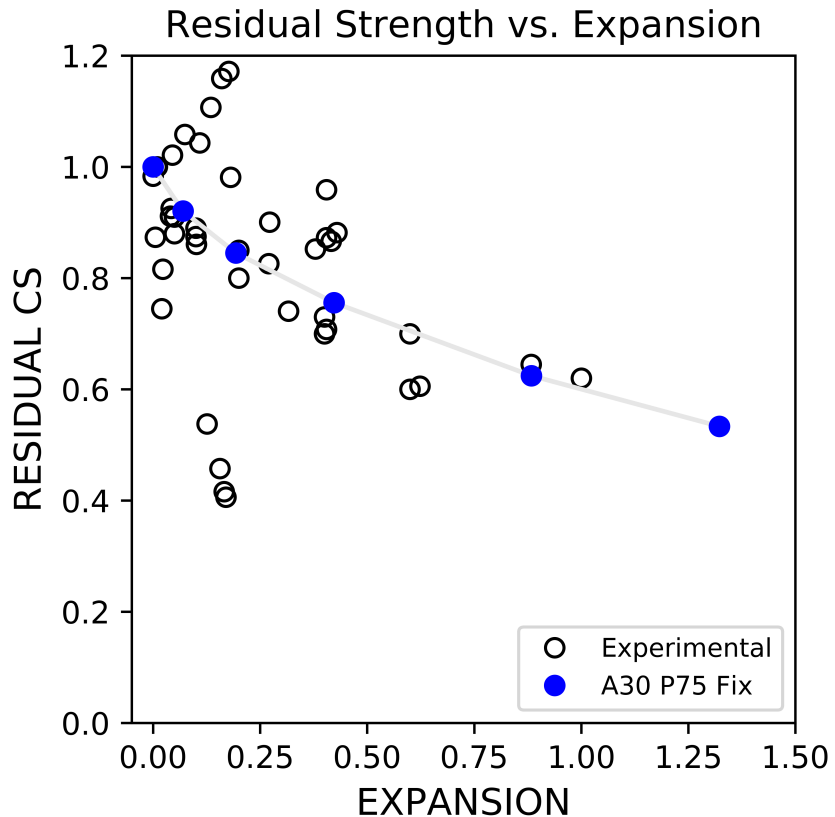


FIGURE 1.34: A30 P75 Compressive Strength Comparing With Experimental Results

However, if plot the residual elastic modulus along with the increasing in expansion, shown in Figure 1.35, the losses in our simulation is significantly higher than experimental result. Start from very low expansion amount the simulated residual elastic modulus dropped to over 80% losses. This implicate that the simulation and for expansion and loading in ASR still requires to be improved to represent the mechanical properties losses more percisely in reality.

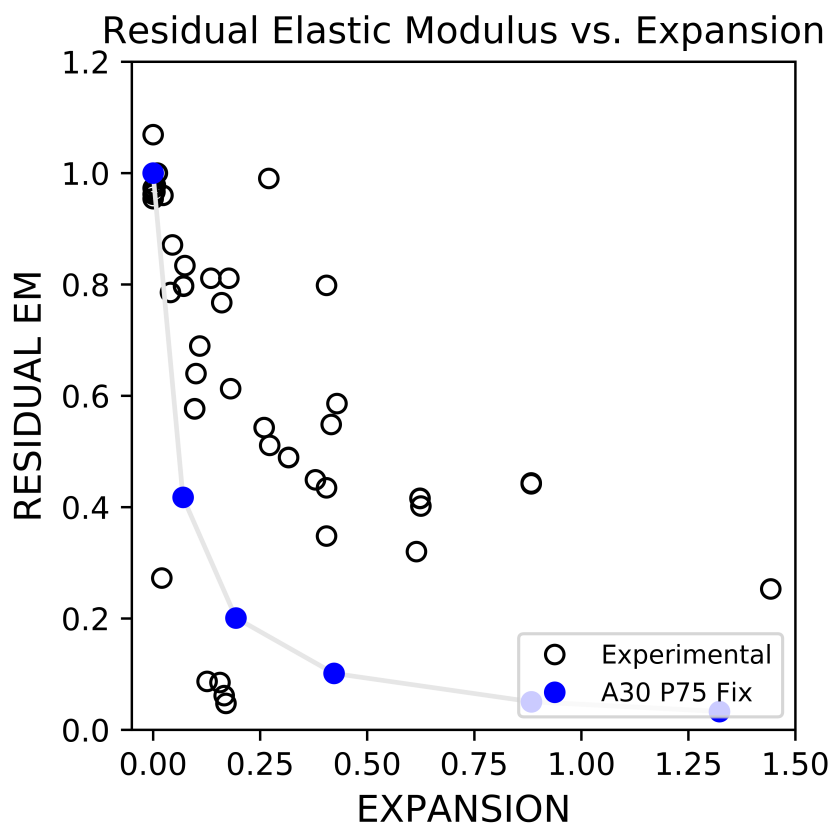


FIGURE 1.35: A30 P75 Elastic Modulus Comparing With Experimental Results

Other uni-axial loading simulation results for expanded models in different cases are also summarized below.

For ASR expanded model with 30% coarse aggregate (of which 25% are ASR reactive), shown in Figure 1.36, the Load-Displacement curve is shown in Figure 1.37.

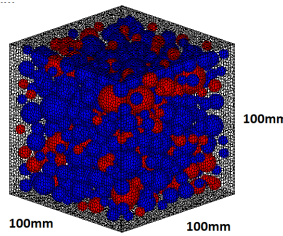


FIGURE 1.36: 30% Coarse Aggregate

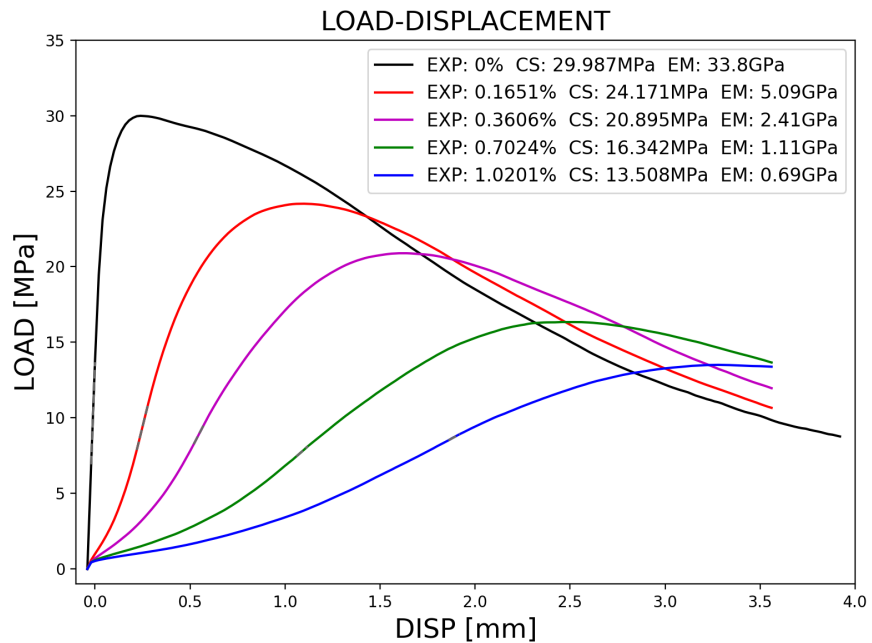


FIGURE 1.37: A30 P25 Fix Load-Displacement

For ASR expanded model with 15% coarse aggregate (of which 75% are ASR reactive), shown in Figure 1.38, the Load-Displacement curve is shown in Figure 1.39.

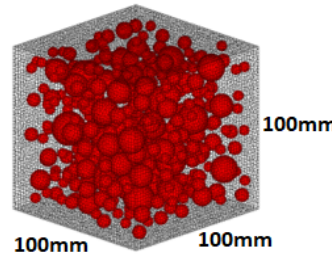


FIGURE 1.38: 15% Coarse Aggregate

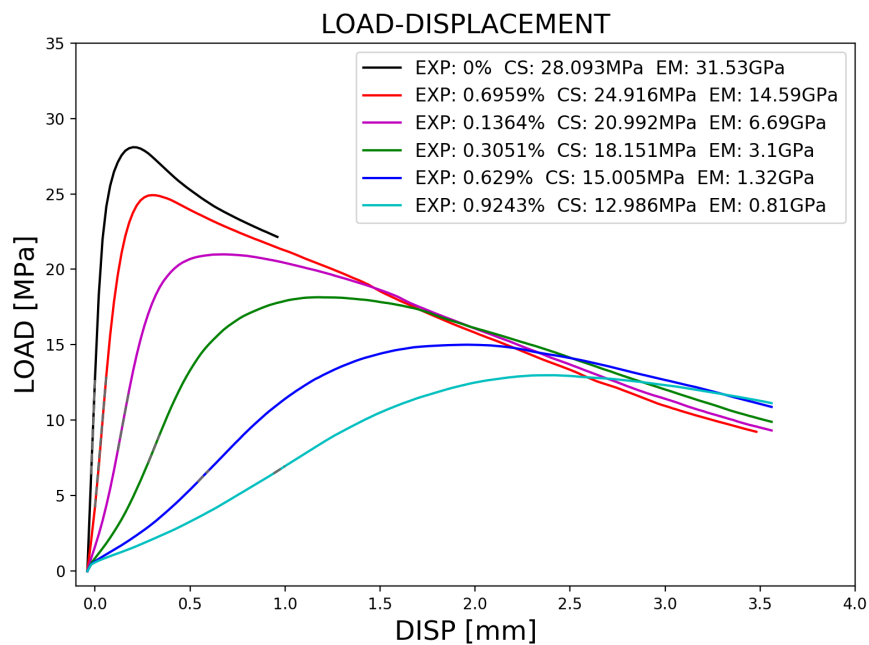


FIGURE 1.39: A15 P75 Fix Load-Displacement

The simulation result in residual compressive strength here is plotted, as in Figure ??, which can be seen that in ASR simulation, the decreasing trend in compressive strength is influenced by factors such as percentage of coarse aggregate, and percentage of reactive aggregate.

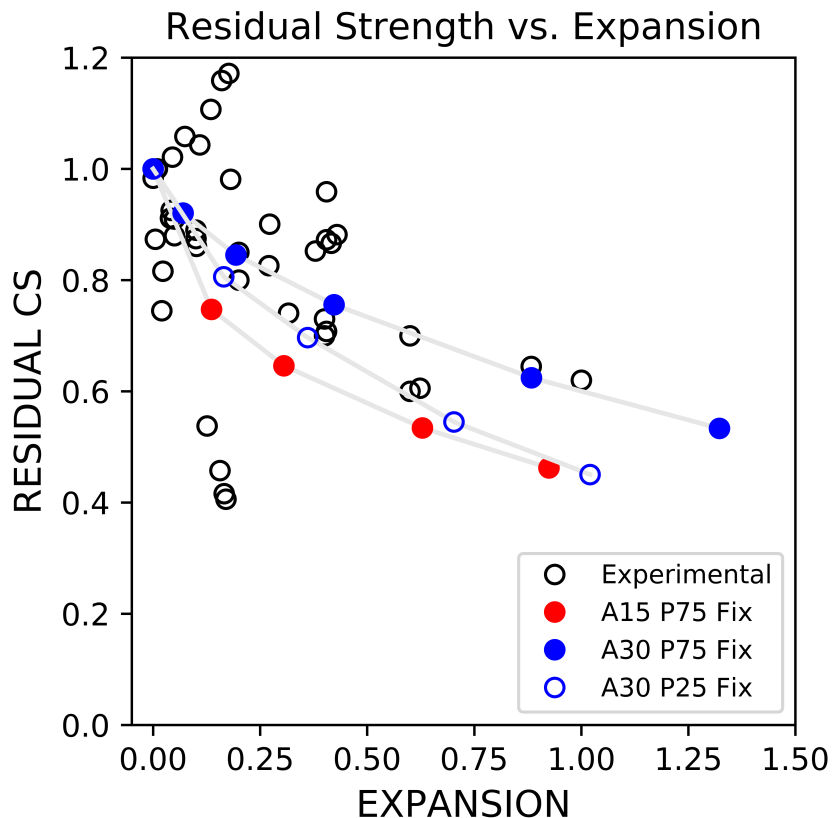


FIGURE 1.40: ASR Compressive Strength Comparing With Experimental Results

When looking at fix boundary loading, the simulation result shown in Figure 1.40 is relatively close to some of the experimental results, as all experimental results here were loaded with fixed boundary condition.

In Figure 1.41 it can be seen that the early losses in elastic modulus is significantly higher than experimental result for all cases, which indicate that further adjustment may required in material properties of expansion damaged concrete model.

As shown in Figure 1.42, if comparing 30% coarse aggregate results(of which 75% are ASR reactive), which are labeled as A30 P75, and 15% coarse aggregate results(of which 75% are ASR reactive), which are labeled as A15 P75, it can be seen that the residual compressive strength in 15% coarse aggregate cases are relative lower than the 30% coarse aggregate cases.

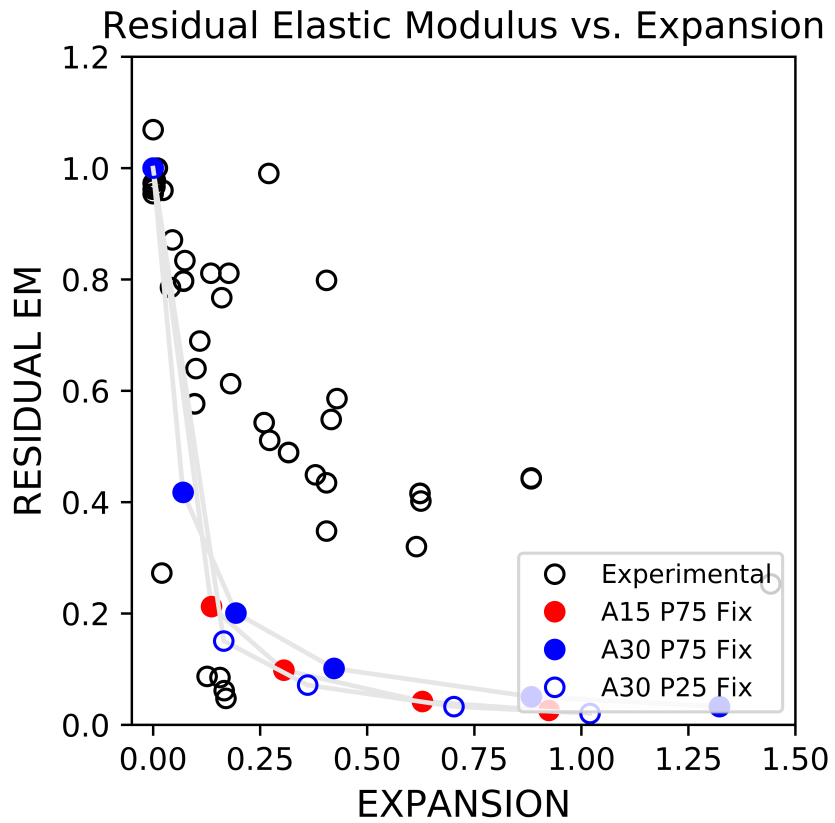


FIGURE 1.41: ASR Elastic Modulus Comparing With Experimental Results

While in Figure 1.43, for the same 30% coarse aggregate cases, if comparing 75% ASR reactive aggregate results, which are labeled as A30 P75, and 25% ASR reactive aggregate results, which are labeled as A30 P25, it can be seen that the residual compressive strength in 25% ASR reactive aggregate cases are relative lower than the 75% ASR reactive aggregate cases.

These differences showing in different ASR expanding conditions implicated that the losses in mechanical properties are not only depends on the level of global expansion. In same amount of global expansion giving, the residual compressive strength can reach a difference up to around 30%. Other factors also have impacts on concretes expanding behavior thus changing the mechanical properties of concrete. In later section, the relationship between cracking distribution in concrete model and its residual mechanical properties will be presented.

Also, the free boundary condition is presented in Figure 1.44, which shows relatively larger losses comparing to the fix boundary condition loading cases. This may due to the cracks generated from the expanding are much easier to open without restrain in the top and bottom boundary, causing larger losses in mechanical properties. However,

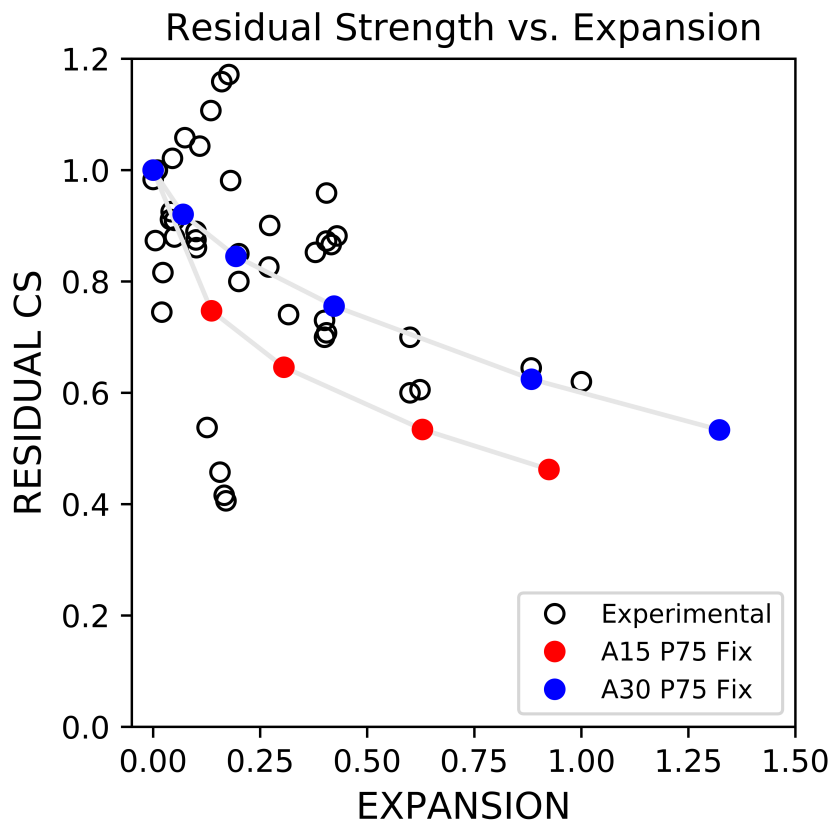


FIGURE 1.42: ASR Compressive Strength Comparing With Experimental Results

the differences in residual compressive strength in different coarse aggregate percentage case are not significant in free boundary condition loading.

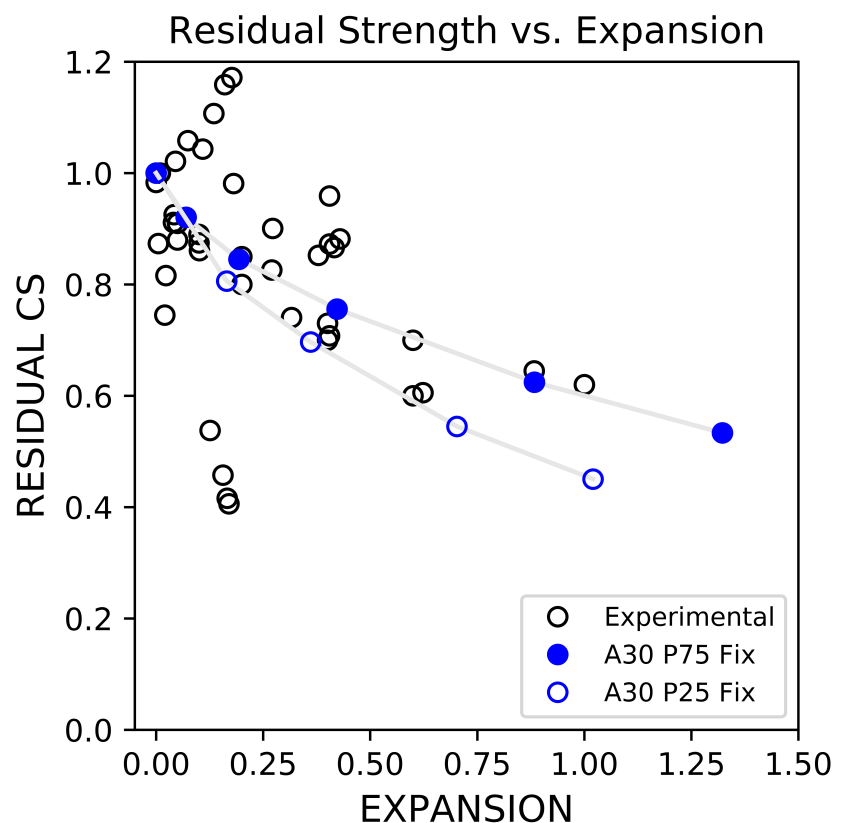


FIGURE 1.43: ASR Compressive Strength Comparing With Experimental Results

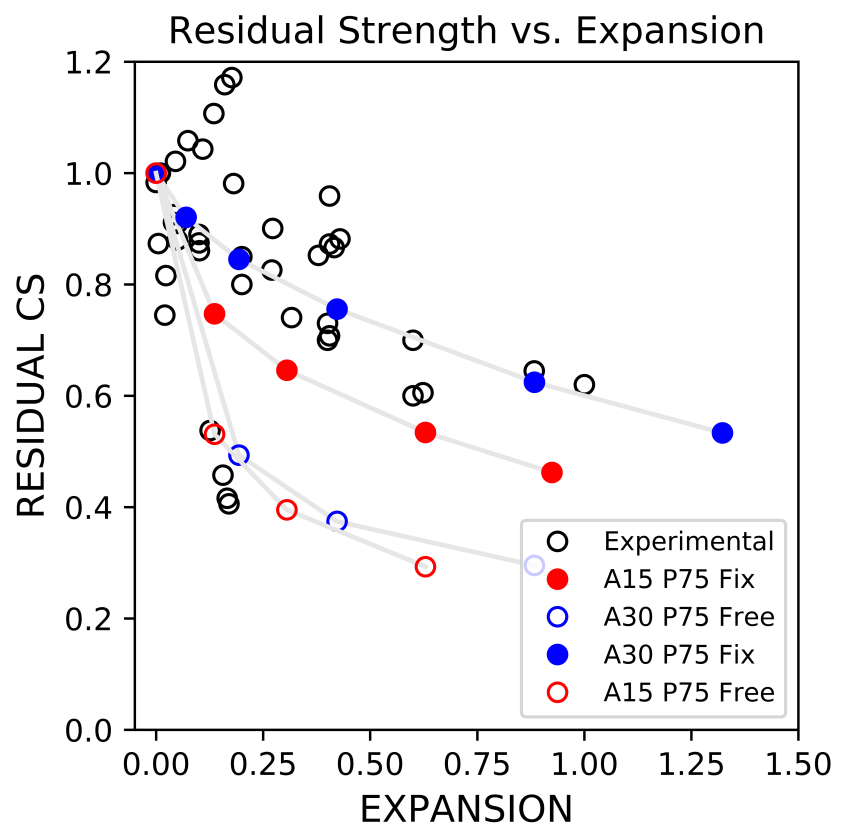


FIGURE 1.44: ASR Compressive Strength Comparing With Experimental Results

1.3.6 Residual Capabilities after Pure DEF Expansion

Similar with ASR loading simulation, uni-axial compression test result for DEF expanded concrete model is summarised.

DEF loading simulation results of intensified center 50x50x50mm (labeled as I50), 75x75x75mm (labeled as I75) and uniformly expansion for all part (intensified center 100x100x100mm, labeled as I100), with aggregate percentage of 30%, are presented. Alternated case for I50 with 15% coarse aggregate is also presented.

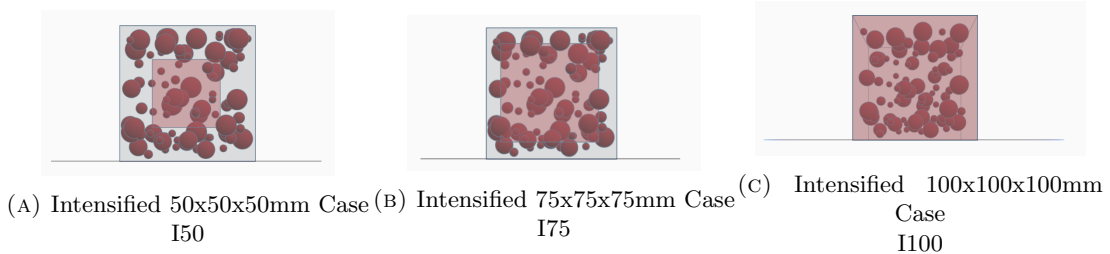


FIGURE 1.45: DEF intensified part range



FIGURE 1.46: Coarse Aggregate Percentage

From Figure 1.47, Figure 1.48, Figure 1.48 and Figure 1.50, Load-Displacement relationships in fix boundary condition uni-axial compression test are shown.

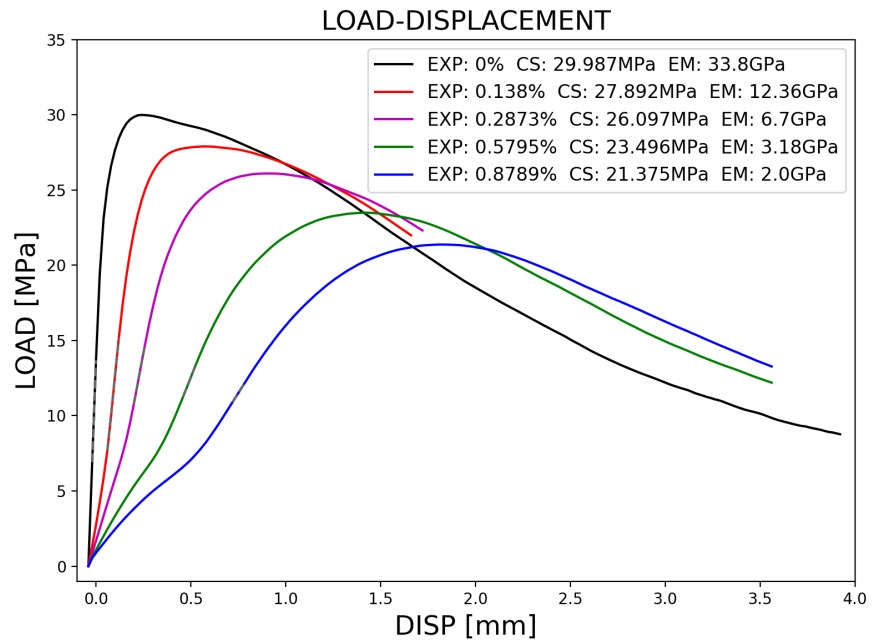


FIGURE 1.47: A30 I50 Fix Load-Displacement

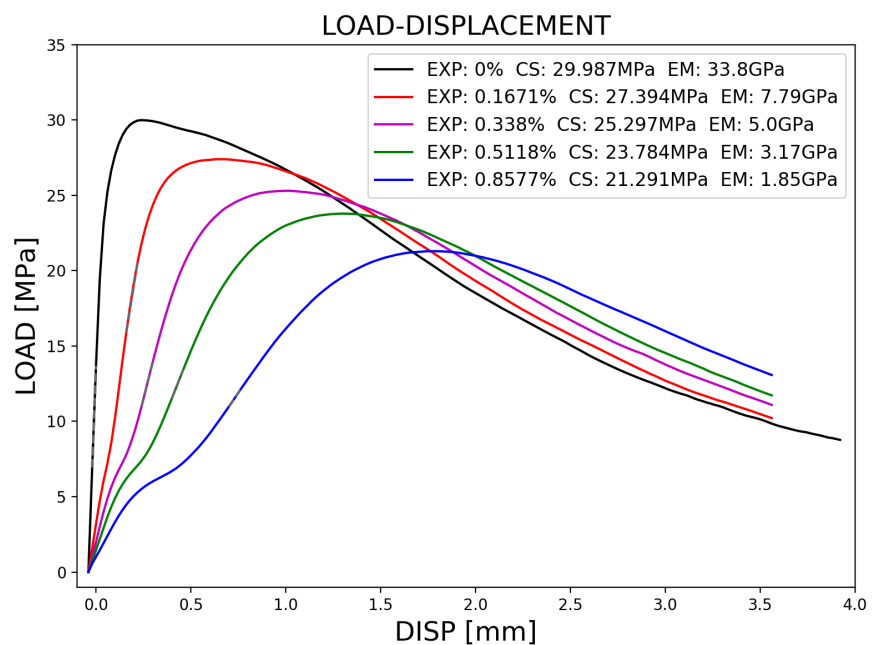


FIGURE 1.48: A30 I75 Fix Load-Displacement

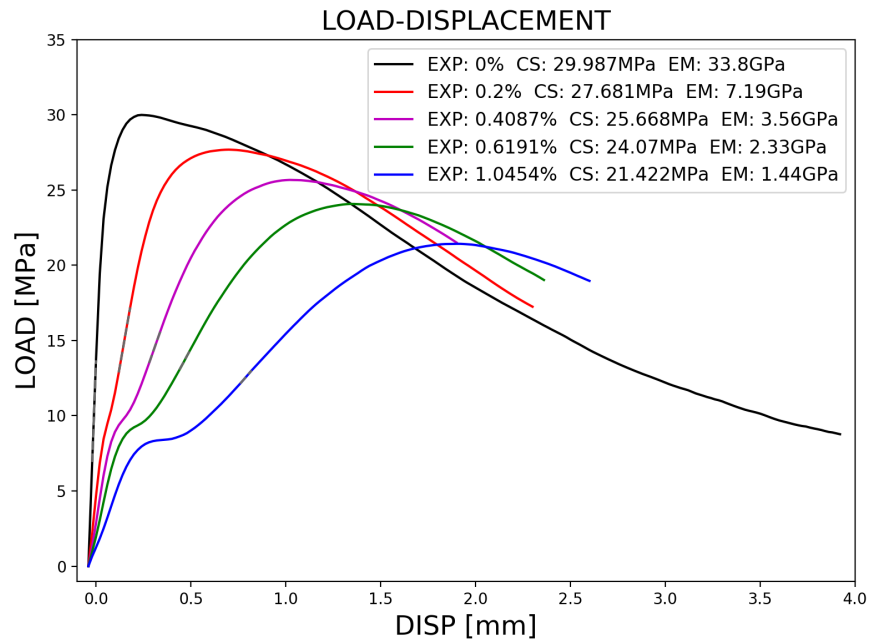


FIGURE 1.49: A15 I50 Fix Load-Displacement

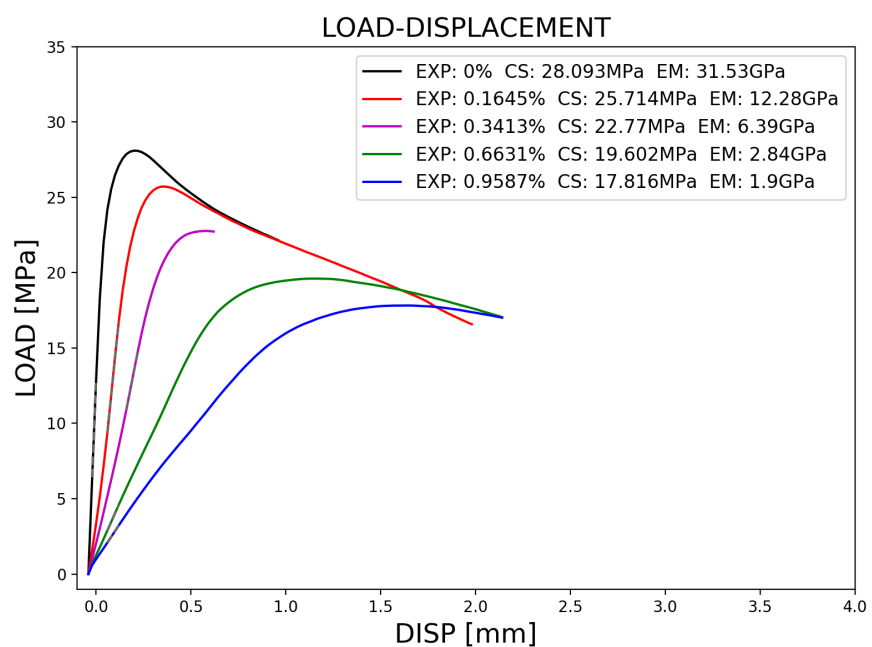


FIGURE 1.50: A15 I50 Fix Load-Displacement

The simulation result in residual compressive strength of DEF damaged models here is plotted, as in Figure 1.51, which can be seen that different with ASR simulation, the decreasing trend in compressive strength is not significantly influenced by factors such as percentage of coarse aggregate, especially the intensified zone range of DEF expansion.

However, same as in ASR expansion elastic modulus simulation results, the residual elastic modulus in all DEF cases are also significantly lower than experimental results. Adjustment in mechanical properties of DEF expanded concrete model may also require modification in further research.

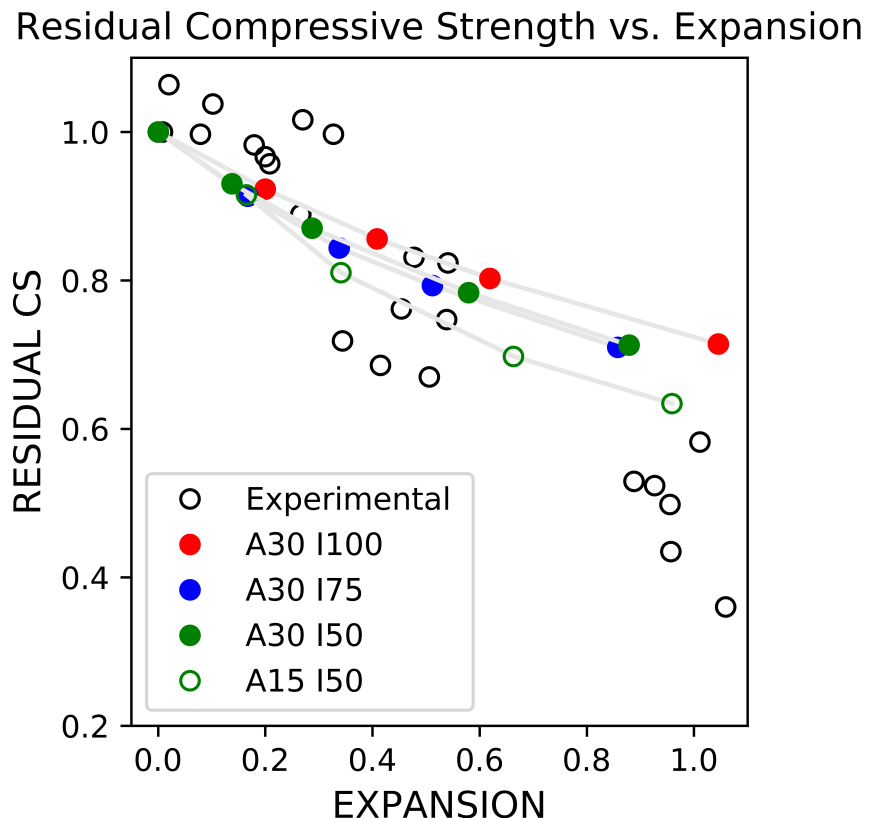


FIGURE 1.51: DEF Compressive Strength Comparing With Experimental Results

In general, the trend in residual compressive strength changing obtained from simulation is not far from the results collected from previous experimental results. With the increasing of global expansion in one-dimensional, compressive strength gradually decrease in all cases.

In some of the Load-Displacement plotting, discontinuity in Elastic Modulus is shown in the loading result, especially in A30 I75 cases and A15 I50 cases. This phenomena is also very common in damaged concrete in reality as the Elastic Modulus would change when cracks are closed horizontally.

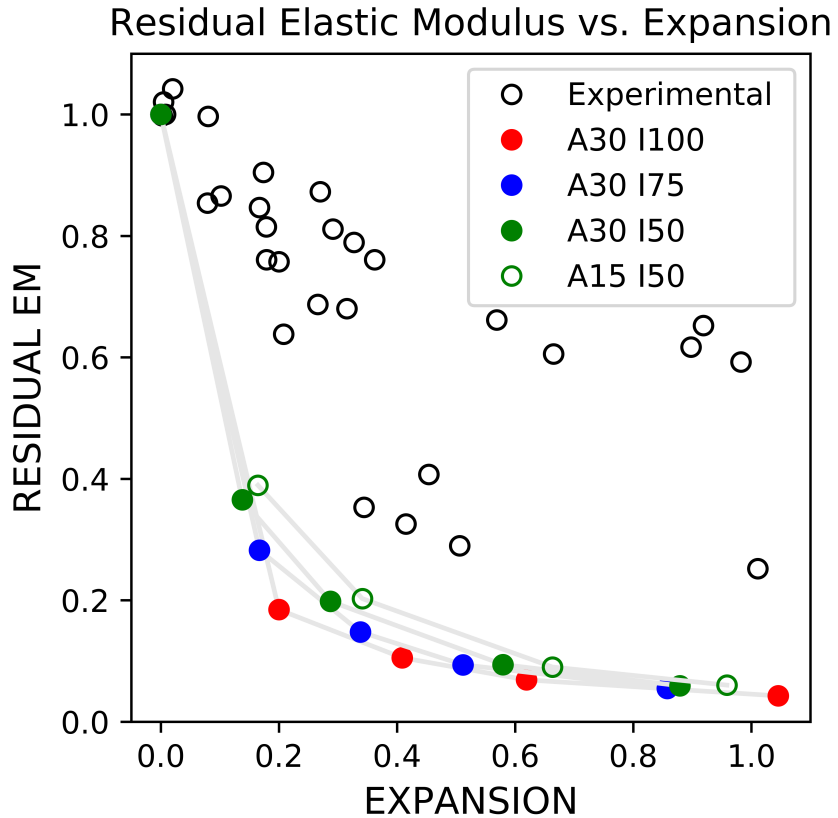


FIGURE 1.52: DEF Elastic Modulus Comparing With Experimental Results

As shown in Figure 1.53, if comparing 30% coarse aggregate results (with center 50x50x50mm zone given intensified DEF expansion), which are labeled as A30 I50, and 15% coarse aggregate results (with center 50x50x50mm zone given intensified DEF expansion), which are labeled as A15 I50, it can be seen that the residual compressive strength in 15% coarse aggregate cases are relative lower than the 30% coarse aggregate cases. However, if compare the residual elastic modulus of A30 I50 and A15 I50 in Figure 1.52, in this time, residual compressive strength in 15% coarse aggregate cases are relative higher than the 30% coarse aggregate cases.

However, the residual compressive strength results for same 30% coarse aggregate models with different DEF intensified zone range are very close. A30 I100 case, as given overall uniform DEF expansion, shows slightly advantage in residual compressive strength comparing to other 2 cases with non-uniformed expansion, but this difference is only around 8%.

While changing DEF expansion intensified zone does change the cracking pattern significantly, the mechanical properties such as compressive strength is not significantly changed.

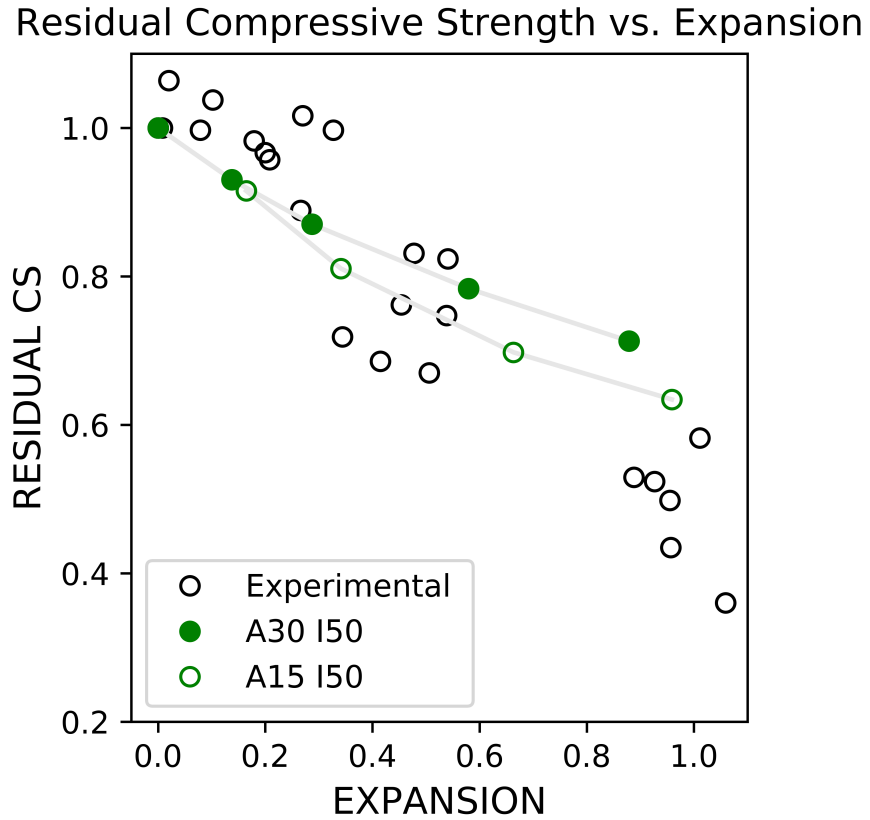


FIGURE 1.53: DEF Compressive Strength Comparing With Experimental Results

However, if cross compare the trend in residual compressive strength and residual elastic modulus, shown in Figure 1.54 and 1.55, it can be seen that the cases with highest residual compressive strength (which is A30 I100 cases here), are having lowest residual elastic modulus. While the cases with lowest residual compressive strength (which is A30 I50 cases here), are having highest residual elastic modulus.

In later section, further discussion of the relationship between cracking distribution in DEF expanded concrete model and its residual mechanical properties will also be presented.

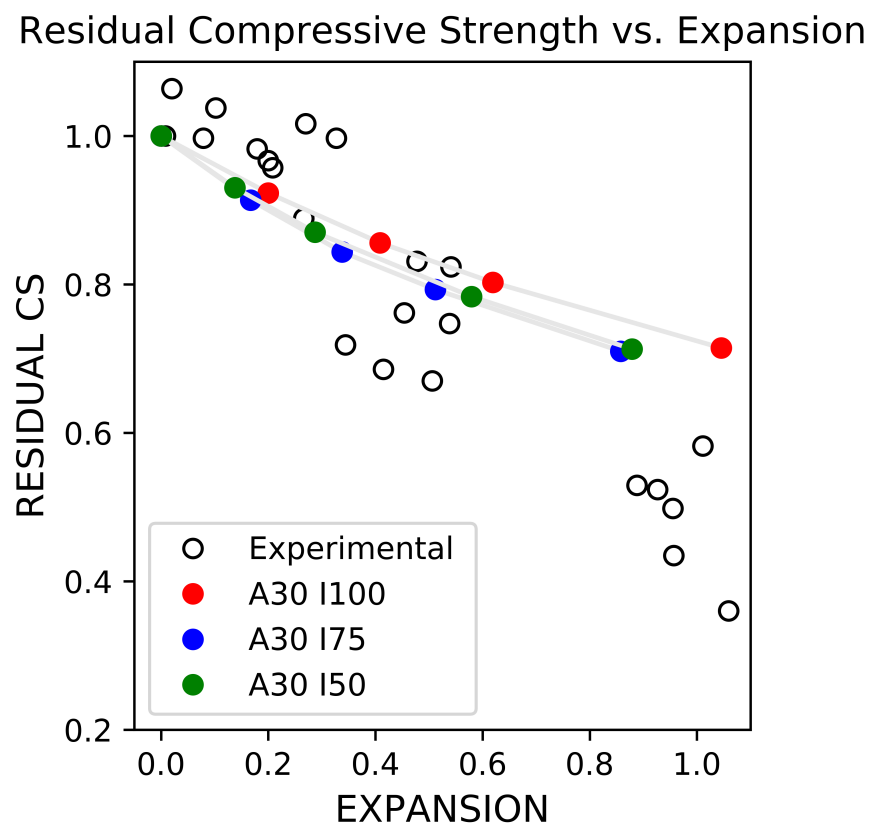


FIGURE 1.54: DEF Compressive Strength Comparing With Experimental Results

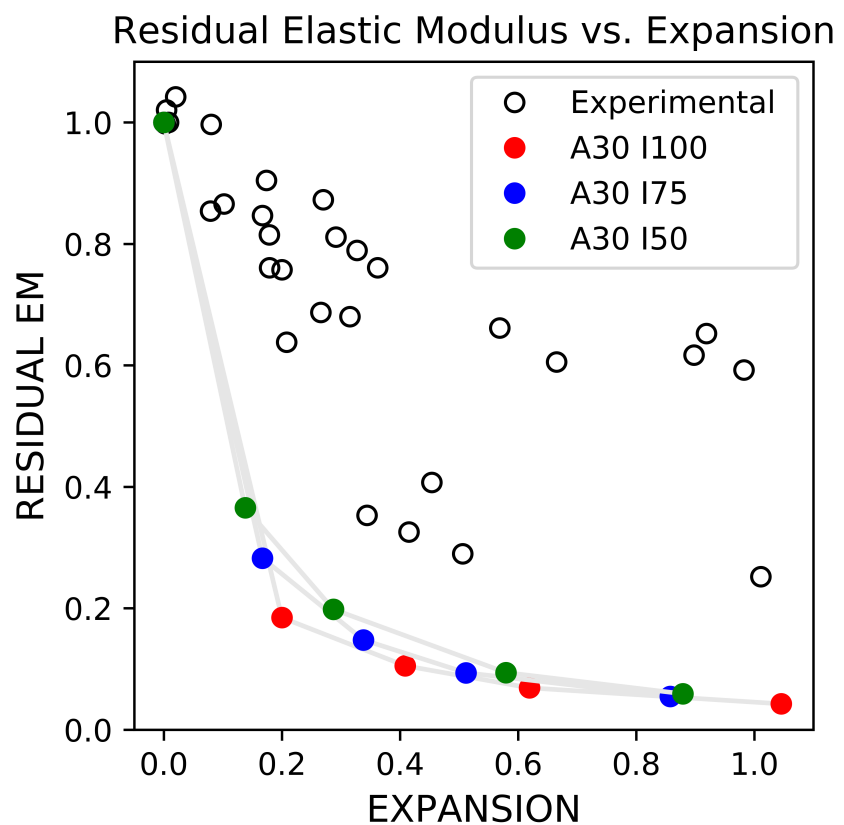


FIGURE 1.55: DEF Elastic Modulus Comparing With Experimental Results

1.3.7 Result And Discussion

In this section, the relationship between concrete's behavior of expansion and its losses on mechanical properties are discussed.

By RBSM, all information of the 3-dimensional cracking behavior can be recorded and analysis numerically. While it is with difficulties to summarized the behavior of expansion by the naked eye, all stress distribution and crack generation process are able to be analyzed numerically.

For example, in Figure 1.56, the relationship of total cracked interfaces and its relationship with residual compressive strength (in a ratio of the compressive strength of undamaged model) is presented.

It can be seen that as the total cracking interfaces number increase, the residual compressive strength decrease in all kinds of expansion applied.

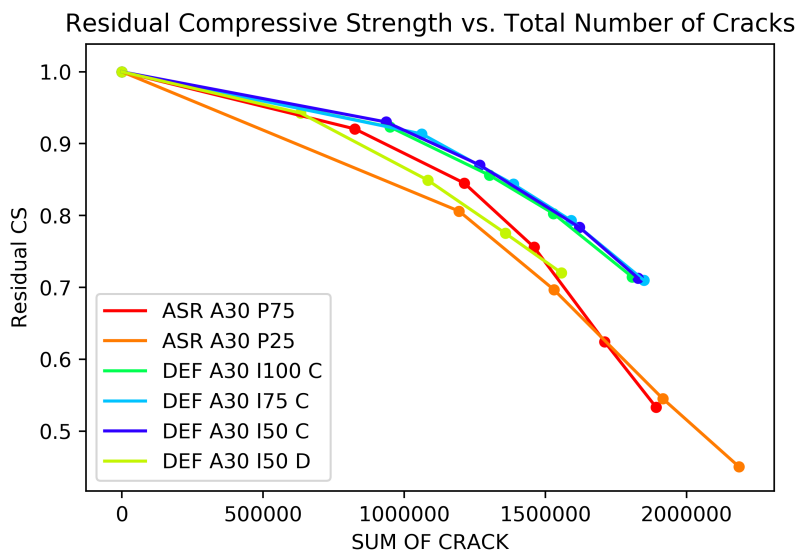


FIGURE 1.56: Residual Compressive Strength vs. Total Number of Cracks

While structually, larger crack in width do represent larger damage, especially in its mechanical properties, here in Figure 1.57 the relationship between total number of cracked interfaces larger than 0.0005mm and the residual compressive strength is plotted.

This time clear linear relationship between the number of cracks larger than 0.0005mm and the reducing in its compressive strength can be seen here, both in ASR expansion and DEF expansion.

This result implied that while the expansion mechanism and cracking pattern can be different in ASR and DEF expansion, the residual mechanical properties, for example,

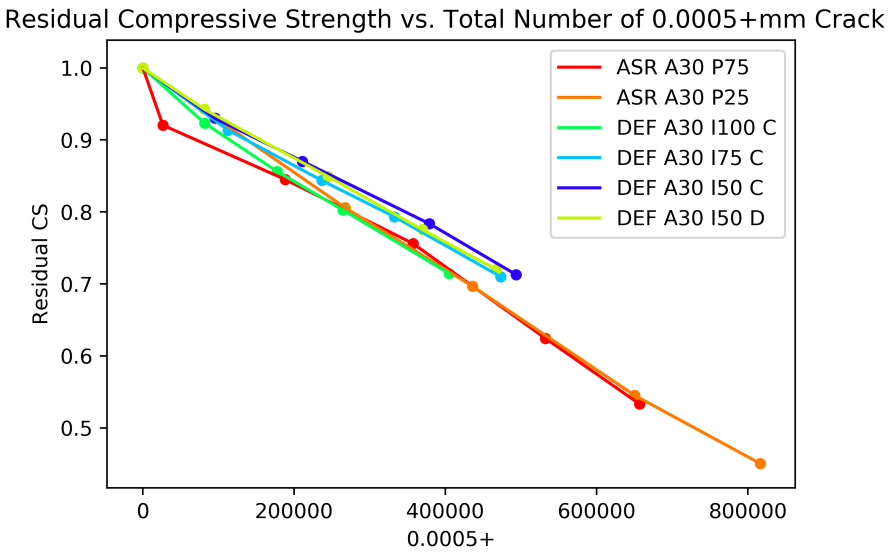


FIGURE 1.57: Residual Compressive Strength vs. Total Number of Cracks over 0.0005mm

the compressive strength, is determined by the existence of larger cracks (0.0005mm+ here). This may offer us a new direction in the analysis the residual capacity of the expanded concrete structure.

Case	Final Expansion	Number of cracked face over 0.0005mm	Residual Compressive Strength
ASR A30P75 Case 3	0.4223	357498	0.7559
DEF A30I50 Case 3	0.5795	379069	0.7835
ASR A30I75 Case 3	0.5118	332827	0.7931

TABLE 1.1: One Dimensional Expansion Ratio in Single ASR Model Simulation

1.4 Conclusion

In this chapter, three-dimensional expanded concrete models are tested under uni-axial compression condition, and the mechanical properties obtained from simulation are compared with previous experimental results from other researchers.

Details about the residual mechanical properties, including residual compressive strength and residual elastic modulus in each loading case for ASR and DEF expansion, are summarized.

The relationships between residual capacity and expansion behavior due to different expansion causes are also discussed.

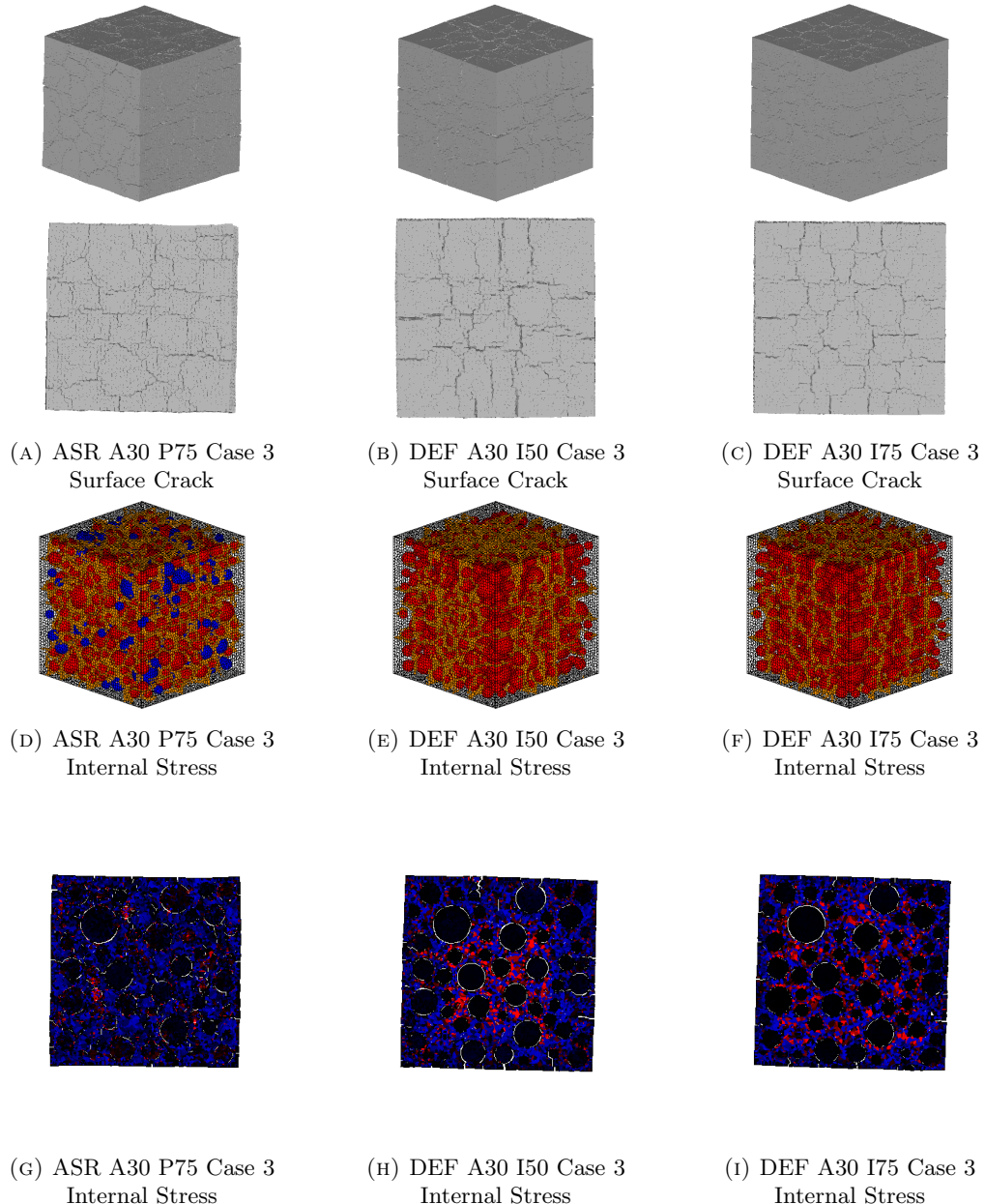


FIGURE 1.58: Cracking Pattern Compare

Linear relationship between the number of cracks larger than 0.0005mm and the reducing in its compressive strength can be seen both in ASR expansion and DEF expansion, implied that while the expansion mechanism and cracking pattern can be different in ASR and DEF expansion, the residual mechanical properties, for example, the compressive strength, is determined by the existence of larger cracks.